Xylem Phenology and Growth Response of European Beech, Silver Fir and Scots Pine along an Elevational Gradient during the Extreme Drought Year 2018

Elena Larysch [1,*], Dominik Florian Stangler [1], Mona Nazari [2], Thomas Seifert [1,3] and Hans-Peter Kahle [1]

1 Chair of Forest Growth and Dendroecology, Faculty of Environment and Natural Resources, Albert-Ludwigs-University Freiburg, Tennenbacher Straße 4, 79106 Freiburg, Germany; dominik.stangler@iww.uni-freiburg.de (D.F.S.); Thomas.Seifert@iww.uni-freiburg.de (T.S.); hans-peter.kahle@iww.uni-freiburg.de (H.-P.K.)

2 Institute of Silviculture, University of Natural Resources and Life Sciences, Peter-Jordan-Straße 82/I, 1190 Vienna, Austria; mona.nazari@boku.ac.at

3 Department of Forest and Wood Science, Stellenbosch University, Private Bag X1, Matieland 7602, South Africa

* Correspondence: elena.larysch@iww.uni-freiburg.de

Abstract: Highlights: European beech (*Fagus sylvatica* L.) and silver fir (Abies alba Mill.) displayed parabolic elevational trends of the cessation of xylem cell differentiation phases. Xylem phenology and growth rates of Scots pine (*Pinus sylvestris* L.) appeared to be less influenced by the 2018 drought, whereas beech reduced growth on the lowest elevation and fir seemed negatively affected in general. Background: The year 2018 was characterized by multiple drought periods and heat waves during the growing season. Our aim was to understand species-specific responses of xylem phenology and growth to drought and how this effect was modified along an elevational gradient. Materials and Methods: We sampled microcores and increment cores along an elevational gradient in the southwestern Black Forest (SW Germany) region and analyzed xylem phenology and growth response to drought. Results: Termination of cell enlargement and lignification occurred earliest in beech and latest in pine. Beech had the highest growth rates but shortest growth durations, fir achieved moderate rates and medium durations and pine had lowest growth rates despite long growth durations. In contrast to pine, onsets of cell differentiation phases of fir and beech did not show clear linear relationships with elevation. Cessation of cell production and lignification of beech and fir followed a parabolic elevational trend and occurred earliest on low elevations, whereas pine showed no changes with elevation. Tree-ring width, generally, depended 3–4 times more on the growth rate than on growth duration. Conclusions: The possibly drought-induced early cessation of cell differentiation and considerable growth reduction of beech appeared to be most severe on the lowest elevation. In comparison, growth reductions of fir were larger and seemed independent from elevation. We found evidence, that productivity might be severely affected at lower elevations, whereas at high elevations wood production might not equally benefit during global warming.

Keywords: cambial activity; tree-ring analysis; elevational gradient; climate change; forest growth; wood formation; lignification; dendroecology

1. Introduction

Climate change-induced drought and heat stress affects forest ecosystems in a complex manner; it impacts its integrity and potential to persist, even in environments that are generally well supplied with water [1,2]. In 2018 a hot drought, one of the most severe and long-lasting summer drought anomaly in combination with heat waves, hit Central Europe. It is claimed that the hot drought in 2018 had a stronger impact on forest ecosystems than the drought of 2003 [3]. The peculiarity of hot droughts lies in the heat wave occurring on top of the drought period, which is boosting the negative effects on vegetation growth [4].

Hence, trees were suffering extreme abiotic stress which was often followed by biotic agents and unprecedented drought-induced tree mortality [5]. It is anticipated that climate change will intensify such hot drought conditions and increase their frequency [5,6].

The ability of trees to stay alive and endure the ongoing climatic changes with its extreme weather events, strongly depends on the capacity of its organs to maintain essential functions, such as the water and nutrient transport [7]. However, changing weather conditions and climate are forcing trees to continuously adjust. Xylem phenology, the crucial timings in the wood tissue developmental phases, is a fundamental response mechanism of trees to adjust and adapt to extrinsic changes and hence, is very sensitive to climate change effects [8,9]. Xylem phenology varies widely between years and shows high plasticity, being controlled by several factors varying throughout the growing season [10–12]. Similar to leaf phenology [13], ambient temperature is the main factor controlling onset of cambial activity and wood formation regardless the elevation and latitude of the site [14–16]. Water supply can play a significant role later in the growing season and cause premature cessation of wood formation, especially at sites which are climatically constrained by low precipitation amounts [17,18]. Water supply thus influences wood formation and resulting wood anatomical properties [19]. Furthermore, the photoperiod is suggested to play a role in controlling the onset and cessation of xylem cell differentiation phases [20], and its effect is also visible in the culmination of the radial growth rate which, in temperate forests, often occurs around the summer solstice to ensure the completion of the maturation of all cells before winter [21,22].

In addition to external factors, intrinsic factors also influence xylem phenology, such as genetics, tree vitality, tree age and/or tree size [21,23–25]. Furthermore, wood formation itself is found to control inherent cell differentiation phases, by cell differentiation phases determining subsequent processes and timings [26].

Increased mortality rates of Norway spruce in many areas of Central Europe are indicative of the maladaptation of this species to the current growing conditions [27]. To secure the climate protection function of temperate forests, long-term strategies are required for the regrowth of the forests after these die-backs with the option of including alternative tree species better suited to the challenges of ongoing climate change [28]. Therefore, it is crucial to understand and compare intra- and interspecific growth responses to environmental stress and climate change under contrasting site conditions [19]. Silver fir (*Abies alba* Mill.), Scots pine (*Pinus sylvestris* L.) and European beech (*Fagus sylvcatica* L.) are native European forests and discussed as possible substitutes for Norway spruce. In context of the negative effects of climate change, the late-successional silver fir is less sensitive to drought compared to Norway spruce [29,30]. Silver fir is an ecologically and economically highly valuable tree species, and an important component of the potential natural vegetation mainly on medium to high elevation sites in Central Europe [31]. Despite the fact that on many sites in Central Europe silver fir seriously suffered under environmental stresses in the 1970 and 1980s [32,33], today it is considered a candidate species with climate change adaptation potential in forest management planning [34–36]. The life strategy of silver fir can be characterized as intensive and efficient with short durations of cell differentiation phases and high growth rates [37,38]. Scots pine as a pioneer species adopts a risky, extensive life strategy with long differentiation of xylem cells and low growth rates in order to gain the lead in accessing new resources [38]. Scots pine is a European key tree species and by its flexible root system and its broad physiological amplitude is considered less sensitive to drought than Norway spruce or silver fir [36,39,40]. However, in some dry regions in Europe, a complex disease phenomenon with heat-drought-associated die-back of Scots pine was already observed [41,42]. There is evidence that silver fir and Scots pine have contrasting leaf phenology and maximum daily rates of tracheid production, but similar timings in xylem phenology [38]. However, up to now, there exist only few observations of the xylem phenology of Scots pine during drought or in xeric environments [43,44]. European beech is the forest tree species which would dominate the potential natural vegetation on most sites in Central Europe [31,45]. Beech is considered sensitive to heat

and drought, however, as the main deciduous tree species important to include in the queue of alternatives for Norway spruce. Beech xylem and leaf phenology was frequently analyzed and compared to conifer species, and can be characterized by later onsets and earlier cessation timings, resulting in a general safer life strategy to prevent frost damage of xylogenetic or tree physiological processes [14,17,46–49]. However, observations of the direct effect of drought on beech wood formation and its phenology are also scarce.

By using elevational transects we intend to observe tree growth along ecological gradients with, typical for the study region, decreasing annual average air temperatures and increasing annual precipitation sums with increasing elevation. Although numerous studies used this research design to monitor and understand the environmental control of wood formation, such as the delayed onset of wood formation with increasing elevation [16,18,38,50], xylem phenology of European beech along elevational gradients and in particular in comparison with silver fir and Scots pine has not, or has rarely been, investigated [44]. An advantage of the elevational gradient is the spatial proximity between the elevational levels guaranteeing highly synchronous weather fluctuations among the sites. An important precondition for the requirements of a "true gradient" [51] is that despite the differences associated to elevation and climate, all other growth relevant factors remain similar such as photoperiod, soil type, species composition and stand structure.

This study contributes an analysis of xylem phenology and growth response of mature European beech, silver fir and Scots pine trees growing along a four-level elevational gradient in the Black Forest region of southwestern Germany during the extreme drought year 2018. We expected no difference in the date of onset and cessation of wood formation between Scots pine and silver fir, but in comparison a later onset and earlier ending and a shorter total duration of wood formation in European beech. In addition, we hypothesized that independent of species, onset of cell production was triggered mainly by spring temperature, thus being delayed with increasing elevation due to decreasing temperature. Moreover, we supposed that the onsets of subsequent cell differentiation phases were controlled by and correlated to the onset of cell production. At lower elevations water availability is a major growth limiting factor due to generally warmer and drier conditions, thus we assume in 2018 trees at low elevations to cease growth earlier, compared to increasing photoperiod limitations at higher elevations. Consequently, the duration of cell differentiation phases would show non-linear relationships with elevation, due to longest durations at the medium elevations mediated by only moderate limitations of temperature in spring and water availability in summer. We expected no differences in the day of maximum growth rate between elevations, as it is assumed to be mainly controlled by photoperiod and to occur close to the timing of summer solstice. Complementary to xylem phenology, we explored possible species-specific responses to drought in the growth rate and tree-ring width and expected similar patterns of water limitation on low elevation sites and photoperiod limitation on high elevation sites. By integrating the information on the timing and rates of tree growth in response to one of the hottest droughts in the region since the beginning of instrumental recordings of climate data, we anticipated novel insights into the responses of xylem phenology and wood formation of three major European tree species in the context of climate change.

2. Materials and Methods

2.1. Research Design and Climatic Conditions

Study sites were selected along a four-level elevational gradient (450, 650, 850 and 1100 m a.s.l.) in the southern Black Forest, close to the city of Freiburg (47°59′41.38″ N, 7°50′59.57″ E; Figure 1). The elevational gradient contains two transects with each replication containing four plots, respectively (Figure 1). The eight northwest-facing plots are mostly situated on clayey gritty slopes and are covered by forest stands dominated by European beech and silver fir with admixed Scots pine trees.
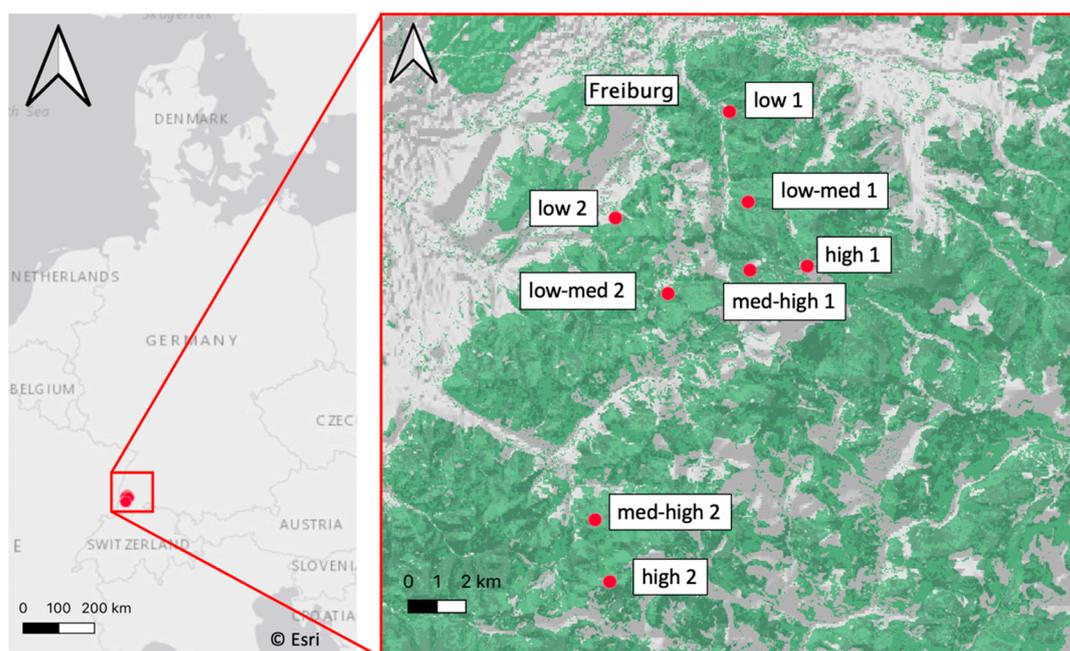
Figure 1. Location of study sites within the Black Forest, southwestern Germany. Plots (red dots) are labelled after their elevational level (low, low-med, med-high, high) and transect number (1 or 2). Digital elevation model provided by [52].

In sum, we selected 66 dominant and co-dominant, vital trees of European beech, silver fir and Scots pine without any visible marks of stem and crown damage. According to the forest stand records, stand age ranged between 70 and 100 years, and on the uppermost elevation beech stand age ranged between 90 and 130 years. On the uppermost elevation, above 1000 m a.s.l., we could not find Scots pine sample trees that met the selection criteria, resulting in the selection of three individuals only for European beech and silver fir within each transect. On the three remaining elevational levels, three individuals of all species within each plot were selected. Tree height and mean diameter at breast height of the sample trees as well as average stand basal area for each elevational level are shown in Table 1.

Table 1. Average stand basal area, sample sizes, mean diameter at breast height (DBH$_{ob}$) and mean tree height with corresponding standard errors at each elevation.

Elevation	Stand Basal Area [m²/ha]	Species	Number of Trees	DBH$_{ob}$ [cm]		Tree Height [m]	
low: 450 m	20.5 ± 1.2	European beech	6	47.7	±1.5	30.2	±1.8
		Scots pine	6	41.3	±1.3	30.5	±1.4
		silver fir	6	51.1	±2.1	25.0	±2.0
low-med: 650 m	24.4 ± 1.9	European beech	6	48.7	±3.4	30.4	±0.8
		Scots pine	6	53.5	±3.5	30.7	±1.0
		silver fir	6	58.8	±3.2	30.6	±1.2
med-high: 850 m	25.3 ± 1.4	European beech	6	35.9	±2.8	24.7	±1.8
		Scots pine	6	42.2	±1.9	24.9	±0.5
		silver fir	6	58.1	±1.8	26.5	±1.1
high: 1100 m	24.7 ± 1.9	European beech	6	31.9	±1.6	23.5	±2.3
		silver fir	6	37.6	±4.4	22.6	±3.8

The study area is characterized by a sub-Atlantic temperate climate with a mean annual air temperature of 7.7 °C and a mean annual precipitation sum of 1394 mm (1968–2018, [53]). The daily climate data were extracted from a spatially interpolated nationwide gridded data set (250 m × 250 m grid) for each of the eight research plots covering the period 1968 to 2018 [54]. The underlying topoclimatological model considers elevation

and terrain exposure index and has been frequently used in modelling forest and tree growth relations with climate before, thus is supposed to comprehensively represent the study sites weather and climates [55–57]. The elevational gradient spans from the lowest to highest elevational level an almost 5 °C mean annual air temperature decrease and a 700 mm annual precipitation sum increase (Table 2). The deviations of the mean annual (Figure 2a) and mean growing period (Figure 2b) temperature and precipitation sum for each of the last 20 years compared to the long-term 50-year mean are revealing a highly anomalous warm and dry year 2018, where the growing period was extraordinarily warm with 2.5 K above the long-term average.

Table 2. Mean annual air temperature (T_{air}) and cumulative precipitation sum (P) and the anomalies in the year 2018 compared to the long-term mean for each plot per elevation.

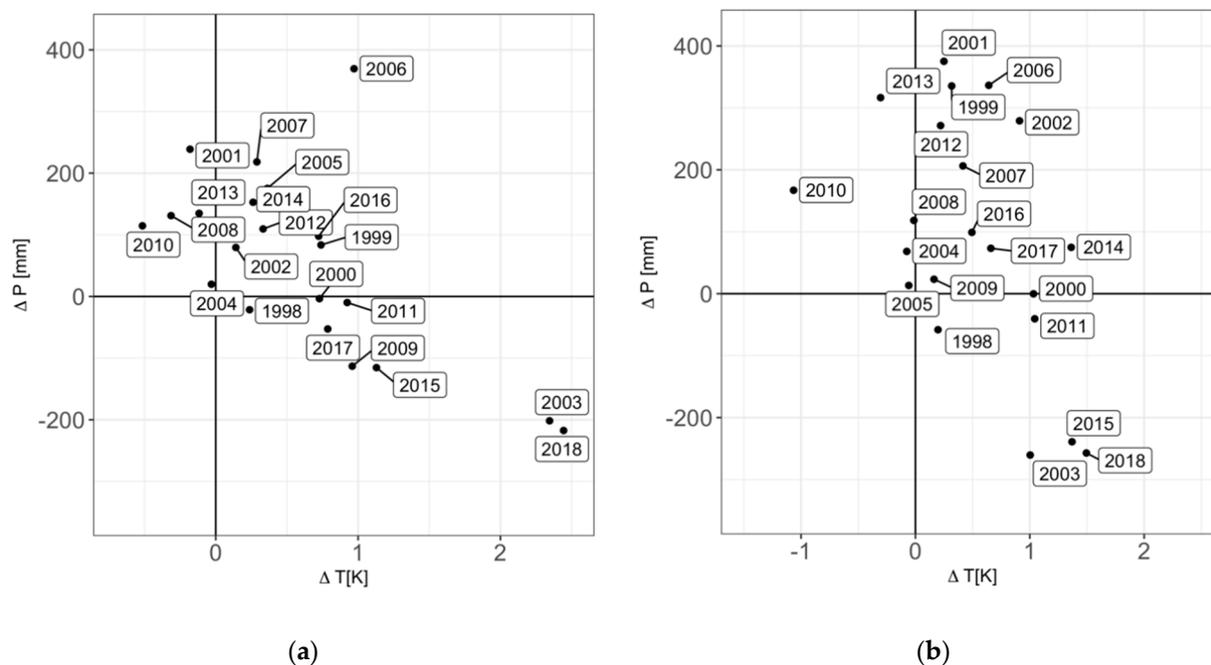| Elevation	Plot	T_{air} [°C]	T_{air} Deviance in 2018 [K]	Annual P [mm]	P Deviance in 2018 [mm]
low: 450 m	1	10.0	+1.4	1072.3	−241.3
	2	9.1	+1.4	1123.3	−223.7
low-med: 650 m	1	8.5	+1.5	1281.8	−197.5
	2	8.9	+1.5	1237.1	−196.9
med-high: 850 m	1	6.6	+1.5	1478.0	−181.6
	2	7.4	+1.5	1554.9	−355.3
high: 1100 m	1	5.9	+1.5	1791.7	−493.4
	2	5.2	+1.5	1616.7	−167.2

(**a**)   (**b**)

Figure 2. Thermopluviograms depicting annual anomalies of mean annual air temperature (K) and mean annual precipitation sum (mm) from the 50-year observation period for the research area (data source: German NFI environmental data base [53]). Horizontal baseline stands for mean annual air temperature, vertical baseline for mean annual precipitation sum. (**a**) Whole year (7.71 °C, 1394 mm); (**b**) growing period (April–September, 12.72 °C, 729 mm).

To characterize the climatic conditions in 2018 in detail, we used climatological and meteorological variables as well as drought indices (Figure 3). To explore the thermal anomalies, we calculated the daily difference of the 2018 daily air temperature to the long-

term mean (Figure 3a). We identified short and long periods of meteorological drought (Figure 3b). The cumulative climatic water balance (CCWB) was calculated based on Haude [57] (Figure 3c). Besides this parameter, we used the monthly Standard Precipitation Index (SPI) to classify and identify droughts [48,58–60] (Figure 3d). To assess and compare the thermal accumulation of the tree species until the onset of wood formation in spring, we calculated the sum of growing degree days (GDD) using daily minimum and maximum temperatures and set T_{base} at 5 °C [61].

$$GDD_{daily} = \left[\frac{(T_{min} - T_{max})}{2} \right] - T_{base}. \tag{1}$$
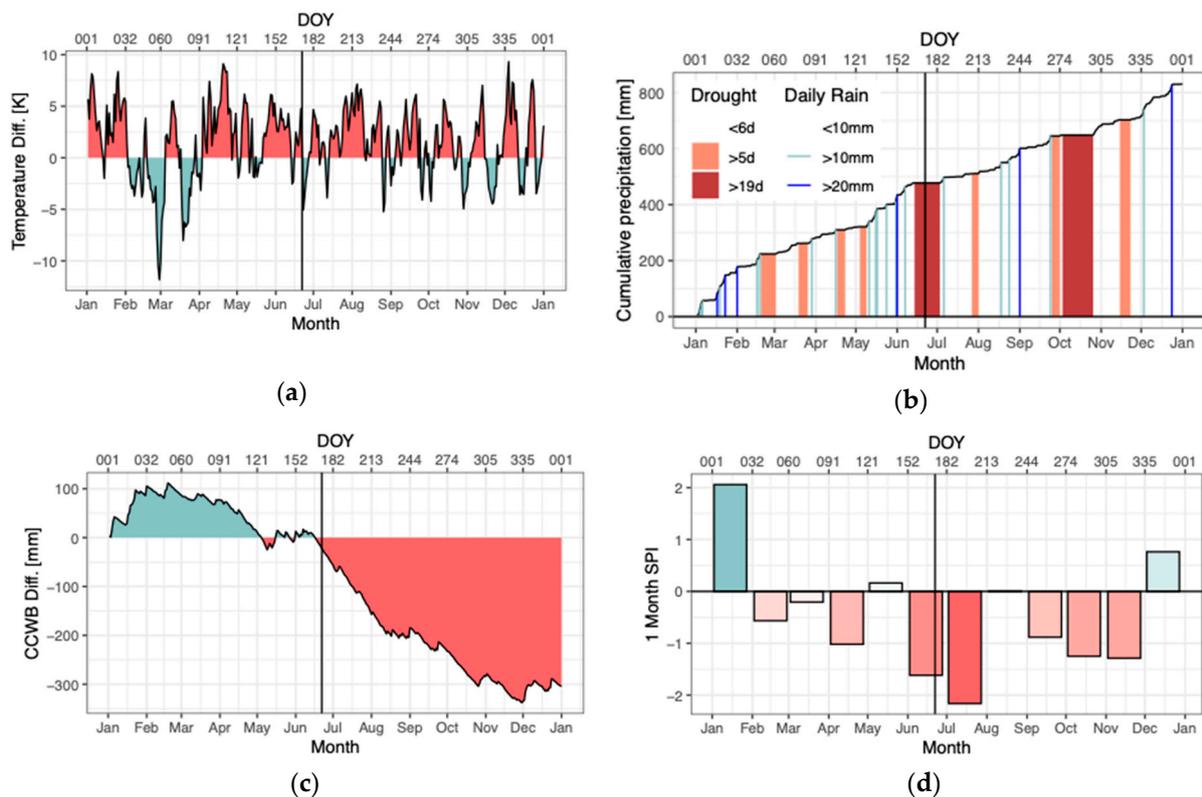

Figure 3. Meteorological and hydrological anomalies in the year 2018 for the low elevation with vertical lines representing the timing of the summer solstice. (**a**) Daily difference of air temperature to long-term mean; (**b**) daily cumulative precipitation sum with underlying rain free periods and daily heavy rain events; (**c**) daily difference of cumulative climatic water balance (CCWB) to long-term mean; (**d**) monthly SPI-values.

If GDD_{daily} was below zero, it was set to zero. For each tree and year, the daily GDDs were summed up from the first day of the year to the day of the first observed xylem cell enlargement.

2.2. Field, Laboratory and Statistical Analysis Methods

Xylogenesis was observed from March to December 2018. Microcores were sampled at breast height (1.3 m) in a weekly to 10-day interval using the Trephor tool [62]. On site, the microcores were placed in Eppendorf microtubes in 50% ethanol solution. In the laboratory, the microcores were stored at 5 °C to avoid tissue deterioration. In the preparation procedure, the microcores were dehydrated in stepwise increasing ethanol solutions and embedded in Technovit 7100 (Heraeus Kulzer GmbH, Hanau, Germany). Thin sections were taken with a sledge microtome, stained with cresyl violet acetate and mounted with Euparal [63]. With support of a Nikon Eclipse Ni-E transmission light

microscope (Nikon Corporation, Düsseldorf, Germany), each sample was studied in visible and polarized light to detect and count cells in the different phases of cell differentiation of the developing xylem.

The process of wood formation can be divided into four sequential cell differentiation phases [64–66]: (1) cambial cell division, (2) xylem cell enlargement, (3) secondary cell wall thickening and lignification and (4) cell maturation. Cambial cells are identified as narrow cells, which have a small radial diameter and thin primary cell walls. After the xylem cells are being produced through division by the cambium initials, the newly formed cells are enlarging, and are characterized by a radial diameter, which is at final stage at minimum twice that of the cambial cell radial diameter, but they still have only a primary cell wall. After the enlarging process, xylem cells enter the phase of secondary wall thickening and lignification. Cells in this phase can be detected by using polarized light, since only the semi-crystalline structures of cellulose in the secondary cell walls shine under polarized light. The last phase is the cell apoptosis, where the protoplasm in the cell is decomposed until the cell is dead. The mature, dead cells are characterized by unicolored blue cell walls and missing cell content.

The critical dates of xylogenesis phenophases are the onset (bE) and cessation of cell enlargement (cE), the onset (bW) and cessation (cW) of cell wall thickening as well as the onset of maturation (bM). The onset of cell enlargement (bE) describes the observation of the very first produced xylem cell in the growing season. bE occurs minimally later than the start of the cambial cell production. The onset of cambial activity is unclear to identify by using light-microscopic methods exclusively [67]. To guarantee the comparability to other studies, we substitute the dates of cell enlarging as dates of cell production, even if a possible time lag between the actual onset of cambial cell divisions and cell enlargement causes a slight bias [18,21,68]. The onsets of the phases were set as soon as 50% of the monitored cells were found present in those phases. The cessations of the phases were set as soon as 50% of the cells were found absent in those phases. Besides the critical dates, we computed the corresponding total durations of cell differentiation processes. The period (ΔE) of cell enlargement was calculated as the number of days between onset and cessation of cell enlargement, the period (ΔW) of cell wall thickening was calculated between onset and cessation of wall thickening and the growth duration (ΔX) was calculated between the onset of cell enlargement and the cessation of wall thickening. To assess the timing and rate of the maximum daily growth, we fitted generalized additive models with monotonically increasing shape constraints to the total number of cells in conifers or the cumulative radial growth in beech as a function of the day of year [69,70]. The timing and rate were then derived by calculating the first-order differences of the predictions of the shape constraint additive models. Modeling of the generalized additive models as well as all following calculations and data analyses were performed in the R programming environment [71].

To evaluate the elevational and species-specific growth responses to the climate anomaly in 2018, we sampled increment cores from our study trees at breast height and derived resistance indices according to Lloret et al. [72] by calculating the relative deviations of tree-ring width in 2018 from the 5-year pre-drought average.

To test for significant effects of elevation and species on the phenological and growth variables and to examine relationships between the tree-ring width, the duration of wood formation and the daily radial growth rates, we used linear mixed-effects models (LMMs) with random intercepts and a hierarchical random effects part in order to account for the clustered data structure [73]. The model procedures are contained in the package *lme4* [74] in R [71]. First, we examined possible species-specific differences with an LMM based on the following model:

$$Y_{ijkl} = \beta_0 + \beta_1\, S_i + b_{jk} + e_{ijkl} \tag{2}$$

where Y is the response variable, β_0 the intercept and $\beta_1 S$ denotes the fixed effect of the species i. The term b denotes the random effect accounting for repeated measurements of the plots j within the transect k, whereas e refers to the residual error term including the individual tree l.

To test for differences of the investigated species along the elevational gradient and to detect possible interaction effects, the following model was formulated:

$$Y_{ijklm} = \beta_0 + \beta_1 S_i + \beta_2 E_m + \beta_3 S_i \times E_m + b_{jk} + e_{ijklm} \tag{3}$$

where the fixed effects remain as described above, but now including the additional fixed effect of the elevation $\beta_2 E$ with the categorically defined elevational levels *m* and *S x E* denoting the interaction term between tree species and elevation. We used the LMMs to calculate multiple comparisons and extracted estimated marginal means using the *emmeans* package with Tukey's procedure to account for the familywise error rate [75].

For the analysis of tree-ring width as a function of growth rates and the growth duration, we also used LMMs based on tree species subsets with the following structure:

$$TRW_{ijkl} = \beta_0 + \beta_1 X_{ijkl} + b_{jk} + e_{ijkl} \tag{4}$$

where *TRW* is the response variable, $\beta_1 X$ either denotes the period of cell enlargement ΔE and the maximum daily growth rate or the product of the maximum rate and ΔE as fixed effect, whereas the random effect and subscripts are as described above. To analyse the relationship of the tree-ring width and phenology during drought, we used the physical model of annual radial growth with the subsequent sensitivity analysis as described in [38].

In addition, analyses of variance were conducted for all LMMs with support of the *lmerTest* package to test the significance of main and interaction effects [76]. The correlation analysis between critical dates of phenophases was computed by using the *ggpairs* function in the *GGally* package [77]. All model assumptions of normality and homoscedasticity of the residual error terms were validated and confirmed (see supplementary material).

3. Results

3.1. Xylem Phenology

3.1.1. The Species Effect

The ANOVA test of the species effect on the xylem phenological variables revealed significant differences for all variables but not for the onset of enlargement (bE) and the corresponding growing degree days (GDD) (Table 3).

Table 3. *p*-values of ANOVAs based on linear mixed-effects models (LMMs) with xylem phenology and growing degree day (GDD) as response variables, tree species and elevation as fixed main and interaction effects and plot as random effect.

Response	Fixed Effects	*p*	Response	Fixed Effects	*p*
bE R^2: 0.65	Elevation Species Species × Elevation	**0.009** *0.089* *0.051*	cE R^2: 0.58	Elevation Species Species × Elevation	*0.080* **<0.001** 0.433
GDD R^2: 0.54	Elevation Species Species × Elevation	0.104 0.244 *0.065*	cW R^2: 0.65	Elevation Species Species × Elevation	0.399 **<0.001** **0.031**
bW R^2: 0.56	Elevation Species Species × Elevation	**0.020** **0.007** **0.015**	ΔE R^2: 0.58	Elevation Species Species × Elevation	0.125 **<0.001** 0.249
bM R^2: 0.66	Elevation Species Species × Elevation	**0.011** **<0.001** **0.008**	ΔW R^2: 0.63	Elevation Species Species × Elevation	0.119 **<0.001** **0.023**
t_{max} R^2: 0.44	Elevation Species Species × Elevation	0.101 **0.002** 0.131	ΔX R^2: 0.66	Elevation Species Species × Elevation	0.105 **<0.001** *0.053*

p-values in bold <0.05, in italics <0.1, R^2: Coefficient of determination of LMMs.

All species started their radial growth on average around 21st April (DOY 111, Figure 4a). Besides bE, the GDD also differed on average only slightly between the species; pine started at 108 GDD, followed by fir and beech with 117 GDD and 125 GDD, respectively (Figure 4b). The onset of wall thickening (bW) occurred earliest in beech (DOY 123, 10 days later than bE), then in pine (DOY 125, 5th May) and on average 5 days later in fir (Figure 4c). The appearance of the first mature cell differed significantly between the conifers and the deciduous species. Beech completed the first cell in the middle of June (DOY 163), whereas pine and fir started the maturation more than two weeks earlier (Figure 4d). The day of the maximum growth rate (t_{max}) in beech happened around summer solstice (21st June), in conifers t_{max} was reached three weeks earlier (DOY 153, Figure 4e). Even if beech started maturation and culminated its growth latest, it ceased cell enlargement (cE) earliest (23rd August), followed by fir (1st September) and pine (on average 1 month later, Figure 4f). The end of wall thickening (cW), thus the end of carbon allocation in the cell wall, followed cE with a delay of six weeks in the same pattern (Figure 4g). Following the onsets and endings, beech had the shortest duration of the enlargement period (ΔE), cell wall thickening (ΔW) and total duration of xylogenesis (ΔX), followed by fir and pine (Figure 4h–j).
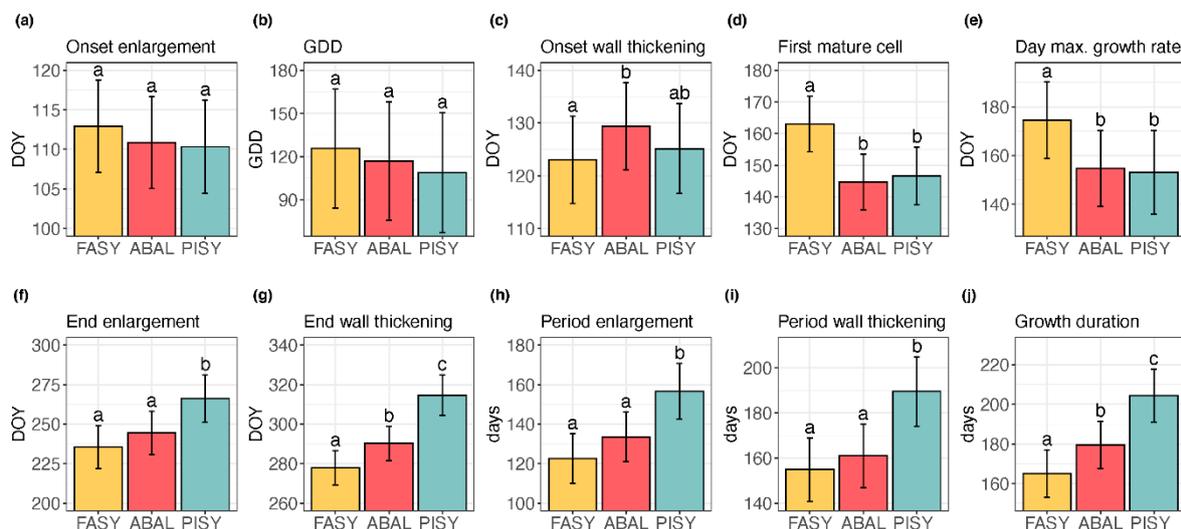

Figure 4. Estimated marginal means of the xylem phenology by species (onset enlargement (**a**), growing degree days (**b**), onset secondary cell wall thickening (**c**), onset maturation (**d**), the day of the maximum growth rate (**e**), cessation of enlargement (**f**), cessation of secondary wall thickening (**g**), the period of enlargement (**h**), the period of secondary wall thickening (**i**) and the overall growth duration (**j**); FASY: *Fagus sylvatica*, ABAL: *Abies alba*, PISY: *Pinus sylvestris*). Error bars indicate 95% confidence levels of estimated marginal means. Different lowercase letters indicate significant differences of the sample means between the tree species ($p < 0.05$).

3.1.2. The Elevational Gradient

The onsets of xylem phenology (bE, bW, bM) were significantly different along the elevational gradient and also the interaction terms between elevation and species were mostly significant (Table 3). In contrast to the species effect, significant effects of elevation on the onsets of cell differentiation phases in spring and early summer were detected, mainly caused by the latest beginnings in the higher elevations (Figure 5a). The significant interaction term can be explained by the parabolic trend in beech and fir, where earliest onsets around the 16th April were indicated not on the lowest but on the second elevation, and the contrasting linear trend in pine with increasing the elevation. The significant positive Pearson correlation coefficients of 0.5–0.75 between the onsets of enlargement, wall thickening and maturation is expressed in the delayed repetition of the pattern of bE in bW and finally in bM (Figure 5b,c). bW in fir was delayed on all elevations about 2–2.5 weeks after bE, only on the third elevation bW was latest and occurred 4 weeks after bE. Beech bW

happened on all elevations about 10 days after bE (DOY 120), on the high elevation on DOY 137. Pine bW was observed on all elevations two weeks after the bE. The elevational pattern in fir was also carried over to the next phenological phase; the beginning of maturation bM (Figure 5c) was, however, slightly less pronounced. For pine the linear trend continued with increasing elevation with bM from mid-May to early June and required continuously more days from bW to bM (17, 20, 28 days). Beech started maturation about 5 weeks after bW, leading to a bM date around 8th of June on all except the upper elevation (26th June). The largest number of growing degree days, about 200 GDD, were indicated for beech and fir on the lowest elevation (Figure 5d); however, differences between elevations were not significant. The day of the maximum growth rate (t_{max}) occurred latest in beech on all elevations around the day of summer solstice (Figure 5e). T_{max} in fir was showing a reverse pattern with earliest peak on the lowest elevation, pines were peaking growth earliest on the lowest elevations as well. Significant Pearson correlation coefficients of all onsets were observed with the day of the maximum growth rate (bE~t_{max} r = 0.46 p = < 0.001, bW~t_{max} r = 0.34 p = 0.004, bM~t_{max} r = 0.6 p = < 0.001).

The end of the cell enlargement (cE) happened earliest in beech (5th August) and fir (11th August) on the lowest elevation with a parabolic trend along the elevational gradient. Pine ceased cell enlargement more than one month later and earliest on the two lower elevations around the 16th of September (Figure 5f, differences between elevations not significant). Concerning the correlation analysis, the beginning of enlargement and the ending of enlargement were not significantly correlated. In beech the cessation of wall thickening (cW) followed the pattern of cE by occurring earliest on the lowest elevation in early September and latest on the third elevation (1 month later), whereas the second and highest elevations were in between (Figure 5g). In fir, however, wall thickening ceased earliest on the highest elevation (7th October) and latest on the second elevation (25th October). Pine ceased wall thickening latest on all elevations between early and middle of November. In regards of the correlation analysis, the earlier the beginning of enlargement (r = −0.4 p = 0.001) or the beginning of maturation (r = −0.49 p = < 0.001), the later was the ending of wall thickening. Additionally, the ending of cell enlargement was positively correlated with the ending of wall thickening (r = 0.65 p = < 0.001).

The period of enlargement (ΔE) displayed in beech and fir a slightly parabolic trend with elevation by having shortest durations at the lowest (3.5 months) and highest (4 months) elevations, respectively (Figure 5h, differences between elevations not significant). In pine trees the enlargement endured longest (more than 5 months) on all elevations and compared with the other species without a clear elevational trend. The trend in the period of wall thickening (ΔW) differed between the species (Figure 5i). In beech, the parabolic trend with longest durations in the mid elevations (5.5 months) was still present. The shortest wall thickening periods in fir (5 months ΔW) and in pine (6 months ΔW) were on the upper elevations. Lastly, the overall xylem growth duration (ΔX) was shortest on the lowest elevation in beech (5 months ΔX) and followed by the parabolic trend already visible in cE, ΔE, cW and ΔW. The xylem growth duration in fir was longest on the second elevation and shortest on the highest elevation. Pine growth duration was slightly longer on the two lower elevations (Figure 5j, differences between elevations not significant).
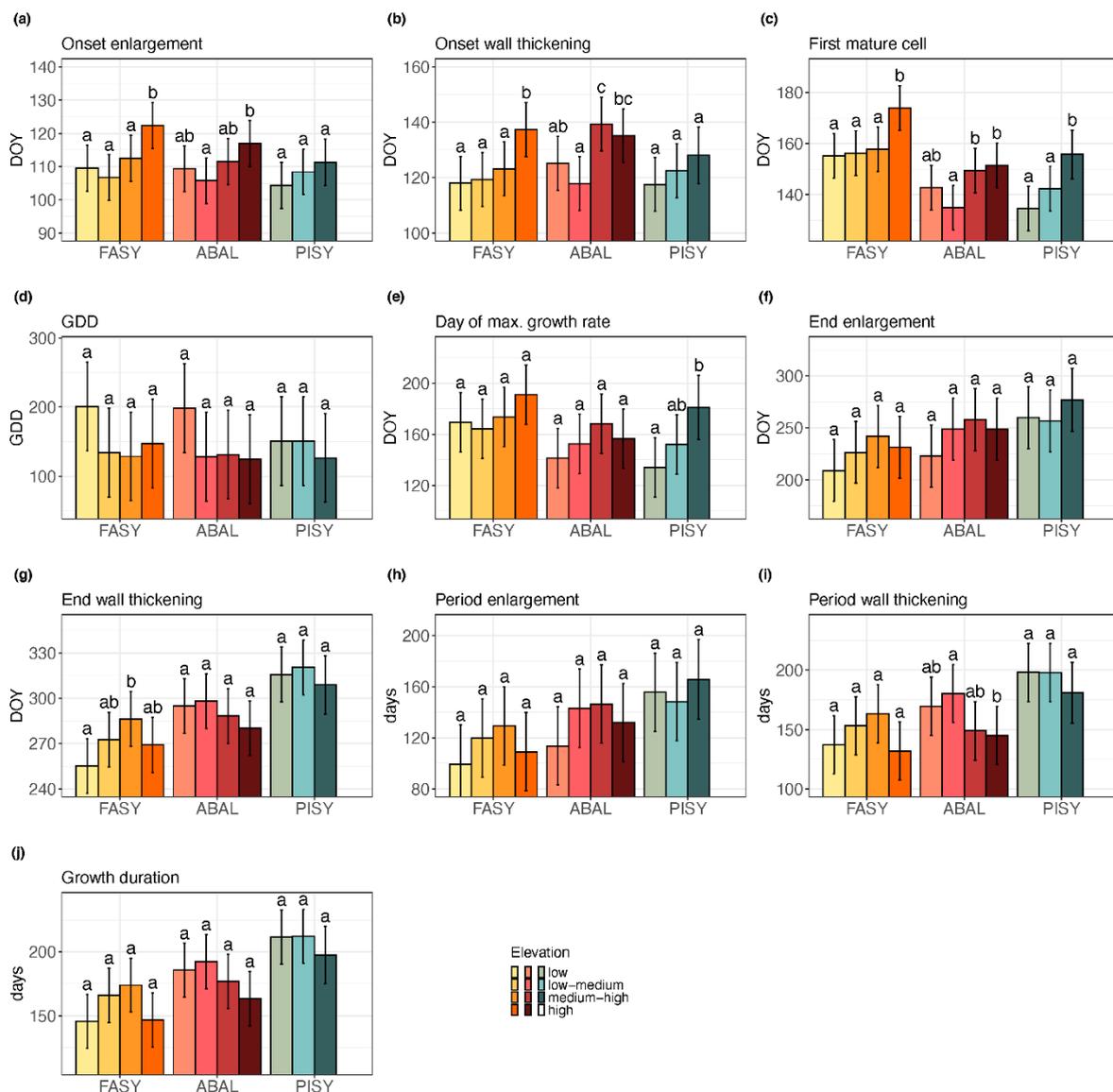
Figure 5. Estimated marginal means of the xylem phenology by elevation and tree species (onset enlargement (**a**), onset secondary cell wall thickening (**b**), onset maturation (**c**), growing degree days (**d**), the day of the maximum daily growth rate (**e**), cessation of enlargement (**f**), cessation of secondary wall thickening (**g**), the period of enlargement (**h**), the period of secondary wall thickening (**i**) and the overall growth duration (**j**); FASY: *Fagus sylvatica*, ABAL: *Abies alba*, PISY: *Pinus sylvestris*). Error bars indicate 95% confidence levels of estimated marginal means. Different lowercase letters indicate significant differences of the sample means between elevations within each tree species ($p < 0.05$).

3.2. Xylem Growth

The correlation analysis revealed a significant positive correlation between tree-ring width and mean daily growth rate and maximum daily growth rate ($r > 0.8$, $p \leq 0.001$). The three variables showed no significant response to elevation, but strong main effects of tree species and interaction effects were detected (Table 4). In Figure 6, the results of the multiple comparison demonstrate that beech had the highest mean and maximum growth rates and the largest tree-ring width produced in 2018, followed by fir and pine. Beech showed also the highest resistance against the drought, followed by pine. Radial growth of silver fir significantly declined in 2018 compared to the other species (Figure 6d).

Table 4. *p*-values of ANOVAs based on LMMs with mean daily growth rate, maximum daily growth rate and tree-ring width as response variables, tree species and elevation as fixed main and interaction effects and plot nested in transect as random effect.

Response	Fixed Effects	*p*
mean rate R^2: 0.52	Elevation	0.704
	Species	**<0.001**
	Species × Elevation	**0.008**
max rate R^2: 0.52	Elevation	0.909
	Species	**<0.001**
	Species × Elevation	**0.035**
TRW R^2: 0.34	Elevation	0.634
	Species	**0.009**
	Species × Elevation	**0.037**
Resistance R^2: 0.40	Elevation	0.159
	Species	**<0.001**
	Species × Elevation	*0.067*

p-values in bold <0.05, in italics <0.1, R^2: Coefficient of determination of LMMs.
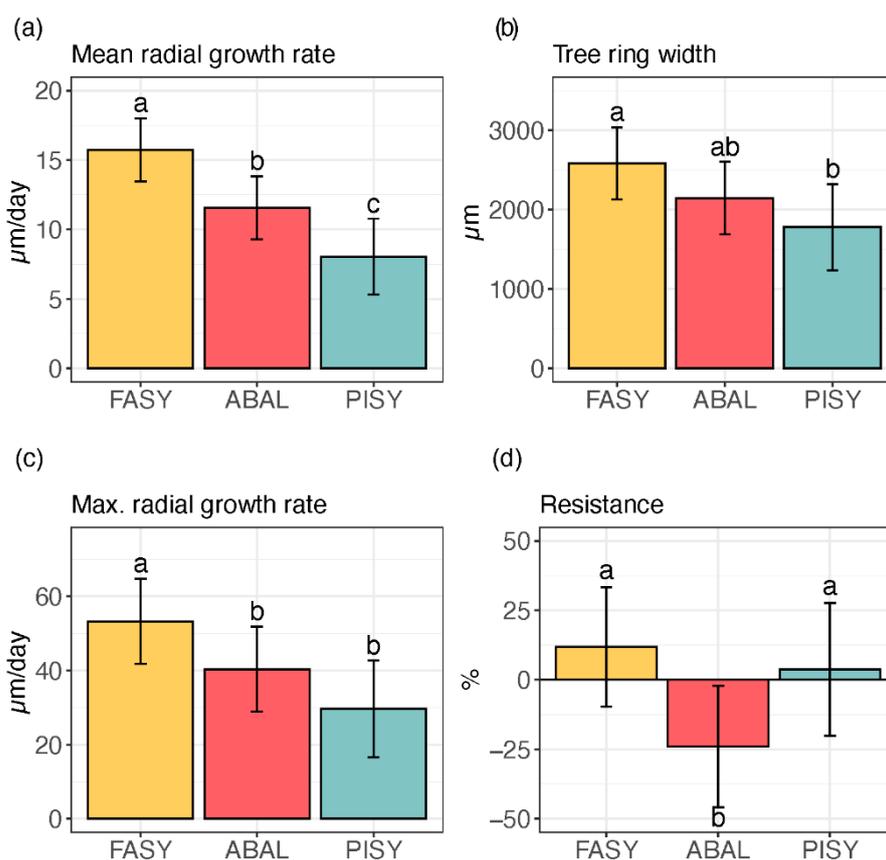

Figure 6. Estimated marginal means of the xylem growth per species (mean daily radial growth rate) (**a**), tree-ring width (**b**); maximum daily radial growth rate (**c**), and the difference between 5-year mean tree-ring width before 2018 and tree-ring width of 2018 (**d**); FASY: *Fagus sylvatica*, ABAL: *Abies alba*, PISY: *Pinus sylvestris*). Error bars indicate 95% confidence levels of estimated marginal means. Different lowercase letters indicate significant differences of the sample means between the tree species (*p* < 0.05).

Besides the significant differences in growth rates between the species, the effect of elevation itself was not significant. However, the significance of most of the interaction

terms was caused by the contrasting effects of elevation within each species, which can be seen in Figure 7, where the variables are split up into each elevational level. Interestingly, the changes along the elevational gradient are similar within each species between all three growth variables (Figure 7a–c). In beech, a parabolic trend is visible, where the highest rates (mean daily 17–19 μm/day and max. daily 62–63 μm/day) and the largest tree-ring width (3018 μm and 3129 μm) were reached in the middle elevations. In fir, a more irregular pattern along the elevational gradient led to highest rates (mean daily 15 μm/day and max. 51 μm/day) and tree-ring widths (2602 μm) in the highest elevation In pine, the rates (mean daily 7–9 μm/day and max. 26–35 μm/day) and tree-ring width (1557–1914 μm) were rather similar between the elevations. The comparison between the tree-ring width of 2018 and the reference period of 2013–2017 revealed a species-specific response to drought along the elevational gradient (Figure 7d). Beech tree-ring width in 2018 decreased significantly only on the lowest elevation by 35%. In contrast, fir resistance was negative on all elevations (-10% to -39%) and growth changes of pine in 2018 compared to the previous years remained small and more static between the elevations (-8% to 8%).
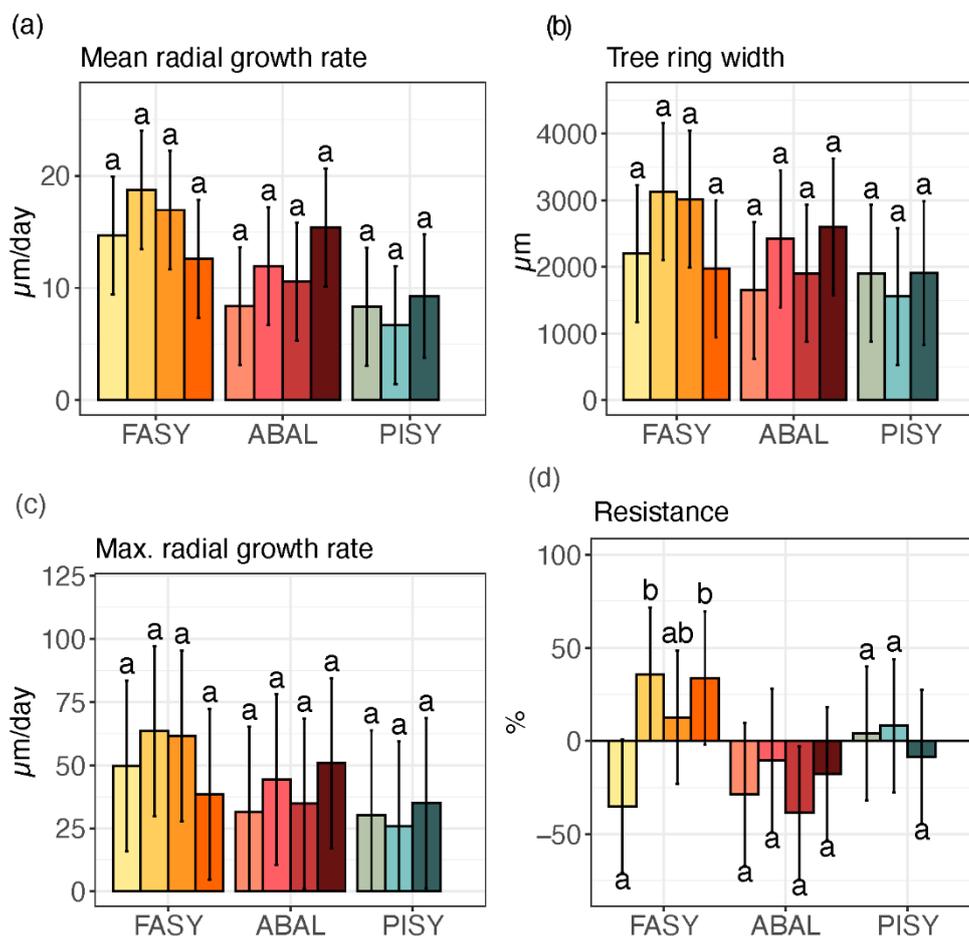

Figure 7. Estimated marginal means of the xylem growth by elevation and tree species (mean radial growth rate) (**a**), maximum radial growth rate (**c**), tree-ring width (**b**) and the difference between 5-year mean tree-ring width before 2018 and tree-ring width of 2018 (**d**); FASY: *Fagus sylvatica*, ABAL: *Abies alba*, PISY: *Pinus sylvestris*). Error bars indicate 95% confidence levels of estimated marginal means. Color legend see Figure 5. Different lowercase letters indicate significant differences of the sample means between the tree species ($p < 0.05$).

3.3. Interaction between Tree-Ring Growth and Phenology

Setting the annual radial increment (TRW) in relation to radial growth duration (ΔE), the maximum growth rate and in relation to the product of rate and duration, a highly

significant, positive linkage is visible (Figure 8). The longer the growth duration, the wider the tree-ring ($p < 0.001$, Figure 8a). Similar patterns were detected for the maximum growth rate ($p < 0.001$, Figure 8b). Furthermore, the radial growth duration significantly increases with the maximum rate ($p < 0.001$, Figure 8c). The tree-ring width is closely linked to the product of rate and duration ($p < 0.001$, Figure 8d). The sensitivity analysis revealed for constant ΔE and varying maximum rate from the mean minus to the mean plus one standard deviation a tree-ring width between 1407 and 3758 µm in European beech, 1117 and 3118 µm in silver fir and 631 and 2932 µm in Scots pine. This results in a range in tree-ring width of 2000–2300 µm with varying rates. Simulating a constant maximum rate and a varying ΔE resulted in the tree-ring width of 2247 to 2919 µm in European beech, 1758 to 2478 µm in silver fir and 1526 to 2037 µm in Scots pine. This results in a range in tree-ring width of 500–700 µm with varying ΔE. If we translate the ranges of the sensitivity analysis in percent, the simulated tree-ring width was 3-times more sensitive in beech and fir and even 4-times more sensitive in pine to changes of the maximum daily growth rate compared to ΔE.
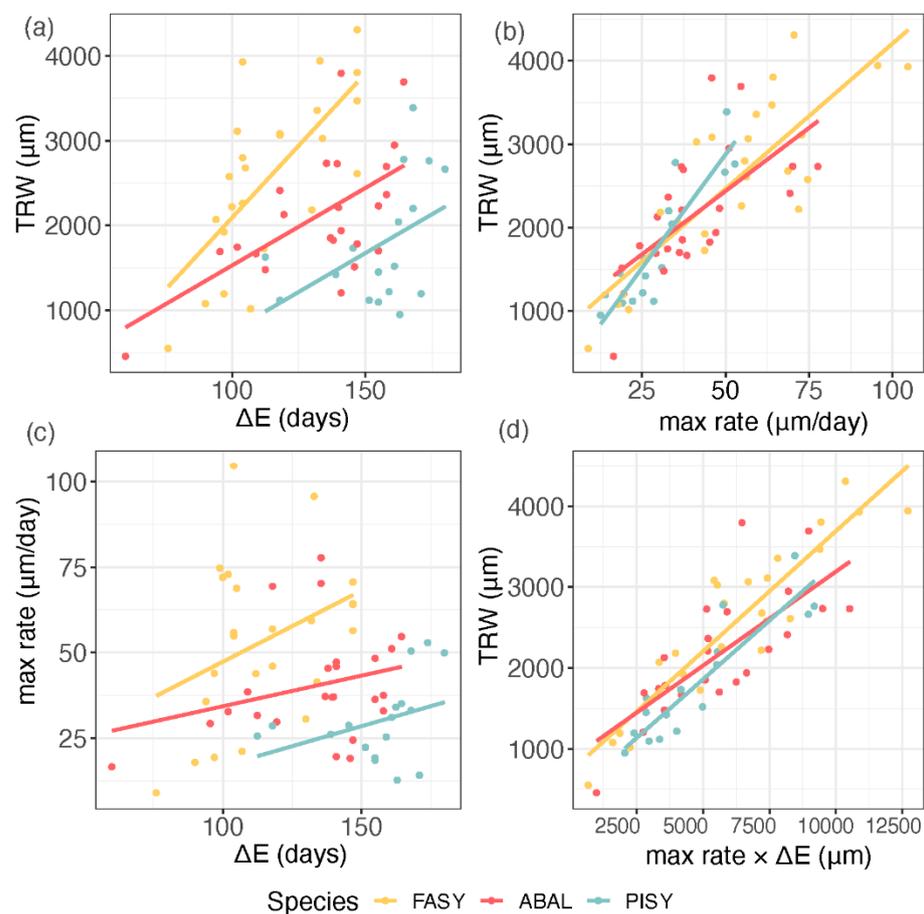

Figure 8. Scatterplots with species-wise linear relationships; (**a**) tree-ring width (TRW) and radial growth duration (ΔE), (**b**) tree-ring width and maximum daily growth rate (µm/day), (**c**) radial growth duration and maximum daily rate, (**d**) tree-ring width and product of rate and duration.

4. Discussion

4.1. Onset of Cell Differentiation Phases and Thermal Accumulation in the Hot Spring 2018

We analyzed xylem phenology and xylem growth related variables of European beech, silver fir and Scots pine along an elevational gradient in the exceptionally dry year 2018. In our study the elevational effect on growth onset was highly significant and can be explained by a universal control of temperature on the reactivation of the cambium after dor-

mancy [15,18,78–81]. Numerous studies demonstrated that spring temperature is playing the major role in the initiation of xylem phenology in temperate forests [16,18,43,68,82–85]. Additionally, heating experiments revealed the positive response of the cambium to artificially increased temperatures in spring [81,86–88]. At lower elevations with a warmer climate, sufficiently high temperatures are reached earlier than at higher elevations [16,80]. This can be seen in Scots pine, where the onset of cell enlargement is earliest at the low elevation, then stepwise delayed along the elevational gradient. Studies comparing tree growth at different elevations showed also that local adaptation of trees to regional climate has an impact on the reactivation of the cambium and the onset of xylogenesis. Trees growing at higher elevations or colder climates needed lower temperature thresholds to start leaf expansion and xylogenesis than trees growing in a warmer climate or at lower elevations [10,89,90]. In our study, European beech and silver fir showed their earliest onsets of enlargement on the second-lowest elevation. This could be explained by higher temperatures and reduced amount of chilling days at the lowest elevation site during the endodormancy phase, resulting in a higher amount of necessary thermal accumulation during the ecodormancy phase and thus possibly delaying the onset of wood formation as underpinned by recent findings [68,91]. Besides such possible ambivalent effects of global warming on xylem phenology, other studies concluded that the interacting impact of mean annual temperature and photoperiod on growth resumption in temperate climates explained most of the variance followed by less pronounced effects of forcing and chilling temperatures [92,93]. If we combine the results concerning the date of onset, the corresponding GDD, the general climate on-site and the climatic conditions shortly before growth onset, we conclude: the threshold of growing degree days for fir and beech was largest at the lowest elevation, but wood production did not start earliest here, resulting in trees obviously not benefitting from the surplus of degree days. The trees growing on the second elevation, however, required less GDD. On the second elevation, the climate is slightly colder and normally we would expect trees to initiate secondary growth later compared with the lowest elevation. Due to a higher amount of chilling days during the endodormancy phase and the warm spring in 2018, less thermal accumulation was needed compared to the lowest elevation. Here, trees might have benefitted from the surplus of spring temperatures and started slightly earlier than on the warmest sites. The higher the elevation, the stronger seemed to be the impact of the general thermal conditions, as trees initiated xylogenesis latest at the highest elevation, even if a similar amount of GDDs was needed as on the second elevation. Our results support previous findings that inter-annual winter and spring temperature fluctuations rather than the tree intrinsic local adaptations are likely the main factors explaining the high plasticity of xylogenesis phenology of our tree species under investigation [68]. Together with the only minimally differing GDD in Scots pine, these findings lead to the conclusion that GDD or forcing temperatures cannot sufficiently explain the growth onset, which was also promoted by other studies [18,94].

Between the species, we did not observe a significant difference in the onset of enlargement, underpinning comparable results of silver fir and Scots pine [38], but contrary to findings were European beech started xylogenesis much later on every elevation than Scots pine [17].

The elevational effect on the onset of all cell differentiation phases (bE, bW, bM) was also found in other studies [16,18,95]. Besides the strong positive correlations of bE, bW, bM, we often found equal time steps along the elevational gradient between the onset of one cell differentiation phase to the next one. This can be explained by the biological process of cell differentiation, where cells need to remain for a certain time in the phase of cell enlargement until they start with secondary cell wall deposition and lignification [65,96]. Consequently, the start of xylogenesis acted as a strong driver of all following processes in wood formation, which confirms previous findings that the onsets of all cell differentiation phases are closely connected [90,97,98]. European beech trees needed less time to finish the enlargement process of the first xylem cells compared to conifers. This can be explained by the different xylem structures between deciduous and coniferous tree species: fiber cells in European

beech are, compared to coniferous earlywood tracheids, rather small and reach their final size rather quickly, whereas extrinsic factors mainly affect the size and distribution of the vessels [99–101]. Interestingly, maturation in European beech started much later than in conifers, resulting in fiber cells remaining comparably long in the phase of wall thickening and carbon allocation despite their small size. The fiber tissue of European beech has rather static intra-annual characteristics and provides mainly mechanical support [102]. Therefore, the relationship between cell wall thickness and cell lumen of fiber cells is more comparable to transition wood or latewood cells of conifers, which need a considerably longer duration of secondary wall formation than earlywood cells [26,103]. Studying the kinetics of cell differentiation of broadleaved tree species could provide additional insights, but this has not been conducted so far on the level of individual vessels or fibers due to the complex wood structure incompatible with the available modeling approaches [104]. Furthermore, secondary wall thickening and lignification of vessels in oriental beech (*Fagus orientalis* Lipsky) was prioritized during xylogenesis, explaining possible time lags in completing cell formation of the surrounding fiber tissue as well [105]. Silver fir needed more time to enlarge their first cells on upper elevations compared to lower elevations. This could be due to the effect of the generally colder climate on the upper elevations, slowing down rates of wood formation processes and triggering compensatory mechanisms by an increased duration of cell differentiation processes in order to maintain hydraulic efficiency and structural reinforcement of individual cells [106]. The lower elevation fir trees could also have expressed a first drought stress signal, since the average delta of the cumulative climatic water balance fell below zero after this date and the trees might have responded with a premature onset of secondary cell wall formation as a mechanism to reduce risks of cavitation and embolism in times of a reduced cell turgor due to the lack of soil water availability.

4.2. Cessation and Duration of Cell Differentiation after the Summer Drought 2018

Trees also need sufficient time to ensure completion of the cell differentiation process for transition wood and latewood cells before onset of winter [10,15,21,107]. Therefore, in a year without a severe drought period, growth cessation is generally assumed to be mainly triggered by photoperiod and should have occurred rather synchronous along our elevational gradient [16,65,91]. However, in 2018, we observed a distinct parabolic trend in beech and fir, in contrast to a linear trend in pine along the elevational gradient. The premature cessation could be explained by hot and dry conditions affecting turgor-driven cell enlargement and cell division processes [41,83,108,109]. Isohydric tree species such as beech, fir and pine close their stomata during periods of severe drought to reduce water loss and to prevent hydraulic failure. As a consequence, reduced photosynthetic activity and concomitant carbon starvation further depletes internal carbon reserves and also negatively affects or even inhibits the production of new cells [1,110–112]. We identified one severe hot drought period without any precipitation starting at 13 June 2018 with a duration of about three weeks and several smaller drought periods between one and two weeks during the vegetation period 2018. This leads to the assumption that silver fir and beech trees on low elevations prematurely ceased their radial increment due to increasing water limitations and carbon starvation; even local temperature was high enough to secure ongoing cell production and cell differentiation completion before onset of winter [18,48,113,114]. In contrast, trees on the less drought-prone high elevations, likely ceased cell enlargement later due to photoperiod limitations, to ensure full differentiation of the lastly formed cells before the first early frost arrives [16,50,80]. That summer drought can cause parabolic patterns of cell enlargement cessation and duration along elevational gradients was also speculated for xylem phenology of European larch in the French Southern Alps [18]. The unusual early cessation of cell production and enlargement at lower elevations of fir and beech is also supported by the considerable reductions of tree-ring width 2018 in comparison to the previous years as tree-ring width/cell numbers are usually closely connected to enlargement duration [23,99,115].

In contrast to previous findings [21], where European beech xylem lignification ceased simultaneously regardless the elevation under average growing conditions, we found the cessation and duration of wall thickening and xylogenesis to vary along the elevational gradient in a similar parabolic pattern as seen for the cessation of cell enlargement, where also the low and high elevation trees were ceasing first. This sequential behavior in cell differentiation phases is controlled by intrinsic factors, which was also observed in other studies [100,105]. Besides the intrinsic control, the carbon demanding process of secondary wall formation in European beech might also have been negatively affected by carbon starvation and the low water availability by the xeric and extreme stressful conditions in a year like 2018 [14,46,100].

In fir, however, wall thickening ended latest in lower elevations and ceasing earlier at higher elevations. The signal in firs of earlier wall thickening cessation at higher elevations might imply a stronger photoperiodical and endogenous control to assure the completion of cell differentiation before winter. In contrast to the onset of wood formation in spring, for which several modeling frameworks were recently published [68,92], the cessation of xylem cell differentiation remains partly erratic, much more complex to understand and demands profound research of the presumably many endogenous and exogenous factors involved [18]. Sample trees growing on the highest elevation sites have slightly higher tree age and reduced tree size, both factors that might have contributed to a more premature cessation of cell differentiation processes [23,24]. While working with natural quasi-experiments such as elevational gradients, it is hardly possible to select study trees, which are identical in size, age and growth history. However, our study shows similar variations in tree characteristics between elevations as a comparable study conducted in the French Southern Alps, who could verify based on subsampling that patterns of xylem phenology of trees were controlled exclusively by elevation and not by tree size or age [18]. To explore ongoing responses of forest ecosystems to climate change, gradient studies remain inalienable tools in climate impact research despite some unavoidable limitations.

Pine might have better compensated the 2018 drought by its generally lower rates of cell differentiation and as indicated by basically no growth reductions in the resistance analysis [104]. In addition, pine could have profited from mild autumn temperatures by ending wood formation significantly later compared to the other species without a clear elevational trend. Scots pine as a pioneer species, following an extensive and riskier life strategy, ceased its cell differentiation processes latest and might be able to benefit from warm autumn temperatures [38,44,116]. In a pan-European study it was found that radial growth of beech was primarily limited in by water availability during summer [44]. Furthermore, in our study, the deciduous European beech followed a secure life strategy and did not profit from the mild autumn temperatures as evergreen conifers possibly do and ended radial increment first. Silver fir, as a climax tree species with an intensive life strategy, ceased radial increment after beech.

4.3. Tree-Ring Width in Relation to Xylem Phenology

It is widely known that xylem growth rates determine tree-ring width [23,38,80]. Under drought, the relative importance of growth rate on tree-ring width is gaining influence compared to the influence of growth duration having highest relative importance under favorable environmental conditions [115,117–119]. The strong positive and significant correlation between the mean and maximum growth rate and the tree-ring width was detected across all investigated species. Furthermore, the sensitivity analysis supported this finding with a 3–4 times stronger dependence of tree-ring width on the growth rate than the growth duration. Cuny et al. found similar results for conifers in France [38].

Different relationships of elevation with growth rates were detected for each species. Scots pine sustained similar growth rates along the elevation. In European beech and silver fir, the lowest growth rates and narrowest rings were found on the lowest elevations, which were most prone to drought. Our findings confirm previous studies on low elevation sites or on sites susceptible to drought [17,48,120,121]. The parabolic trend with increasing

elevation in beech and the slightly similar trend in fir indicate that growth rates of trees in medium elevations of the Black Forest might be less affected by drought periods [80,105]. At least for European beech, this assumption was clearly underpinned by the resistance analysis and highly significant reductions of tree-ring width at the lowest elevation only. Although in 2018 beech showed above-average tree-ring widths at medium and higher elevations, silver fir was not able to profit in high elevations from warmer temperatures through higher tree-ring width increments.

The correlation of tree-ring width and the period of cell enlargement was not significant across species but rather a species-unspecific phenomenon. The period of radial growth was shortest in European beech, followed by silver fir, and longest in Scots pine. Vice versa, the mean and maximum daily radial growth rates and the tree-ring widths were highest in European beech, followed by silver fir, and shortest in Scots pine. European beech and silver fir are both shade-tolerant climax tree species in our study region. Reasons for shade-tolerant species having higher growth rates than pioneer species like Scots pine could lie in their different photosynthetic capacities, resulting in Scots pine producing less assimilates and generally having less dividing cambial cells and longer cell cycles in comparison [38]. European beech had higher growth rates and wider tree-rings than fir probably due to the general need to compensate the relatively shorter growth duration. Other studies also postulated conifers are more prone to form drought-induced narrower tree-rings [122,123]. If we assume a lag effect one year after the drought, this would affect European beech more than silver fir as also found in [124,125]. The strong negative effect of the 2018 drought on wood formation of silver fir on all elevations also challenges conclusions of previous findings, recommending silver fir as a viable forest management option due to its presumed lower sensitivity and higher resistance to drought [30,126].

Under optimal growing conditions in temperature-limited environments, the daily radial increment in conifers is peaking around summer solstice when maximum day length is occurring [22,87]. European beech was documented to maximize daily growth rates up to two weeks earlier [14,127]. In our study, European beech growth culminated around summer solstice and was significantly delayed by three weeks in comparison to the conifer's growth peak. Silver fir and Scots pine peaked xylem growth during the same time, thus simultaneously and intensively competing for resources, whereas the struggle to survive for co-existing conifers is even higher during extreme environmental conditions [38,128]. Furthermore, within each tree, the competition for assimilates between aboveground and belowground organs can lead to premature peaks of the growth rate to guarantee water and nutrient supply for functions relevant for tree survival [129]. Furthermore, due to the increasing heat and water stress in June, the reduced photosynthetic capacity and concomitant shortage of non-structural carbohydrates for biosynthesis of lignocellulose components combined with low turgor pressure could have reduced conifer growth rates already before the summer solstice.

To better understand the full response spectrum of wood formation to variability in weather conditions and water supply, a detailed analysis of the kinetics of wood formation is crucial. Modeling rates and durations of cell enlargement and cell wall thickening can provide additional information on the developmental and environmental control of wood formation processes and possible adaptions on the cell-anatomical level to survive within hot drought periods in a changing climate [107,122].

5. Conclusions

Dry and warm spring conditions, and in particular the three week lasting drought period around summer solstice, had severe and negative impacts on the climatic water balance during the growing season in 2018. A possible drought-induced premature cessation of cell enlargement and growth reduction of European beech appeared to be most severe on the lowest elevation. Furthermore, silver fir showed the earliest cessation at the lowest elevation, but significantly higher growth reductions compared to beech and pine that seemed more independent from elevation.

Interestingly, trees relied also in a drought year mainly on the functional trait "radial increment rate" and less on its duration, regardless of the species and the elevational level. Thus, a prolongation in the vegetation period due to increased temperatures would not automatically induce a substantial increase in wood production or carbon sequestration.

If extreme climatic events, such as the 2018 summer drought, an increase in frequency as projected in future climate scenarios could lead to a widespread reduction of the productivity of several European main tree species, and possibly also European beech, in particular at lower elevations [5,109,130–132]. With our study, we were able to compare responses in the xylem phenology of major European tree species in the extraordinarily hot and dry year 2018 in gradually differing climatic conditions. To consolidate our knowledge of the impact of the drought anomaly on the timings and durations of xylem phenophases and xylem production, longer time series of xylogenesis monitoring need to be established. This would provide more in-depth insights and understanding of the causal relationships between wood formation and environmental changes. This will also provide support for future forest planning to guarantee that forests remain the major terrestrial sink of anthropogenic CO_2 emissions and continue to provide a multitude of ecosystem services.

References

1. Allen, C.D.; Macalady, A.K.; Chenchouni, H.; Bachelet, D.; McDowell, N.G.; Vennetier, M.; Kitzberger, T.; Rigling, A.; Breshears, D.D.; Hogg, E.H.; et al. A global overview of drought and heat-induced tree mortality reveals emerging climate change risks for forests. *For. Ecol. Manag.* **2010**, *259*, 660–684. [CrossRef]
2. Skiadaresis, G.; Schwarz, J.A.; Bauhus, J. Groundwater Extraction in Floodplain Forests Reduces Radial Growth and Increases Summer Drought Sensitivity of Pedunculate Oak Trees (*Quercus robur* L.). *Front. For. Glob. Chang.* **2019**, *2*. [CrossRef]
3. Buras, A.; Rammig, A.; Zang, C.S. Quantifying impacts of the 2018 drought on European ecosystems in comparison to 2003. *Biogeosciences* **2020**, *17*, 1655–1672. [CrossRef]
4. Yuan, W.; Zheng, Y.; Piao, S.; Ciais, P.; Lombardozzi, D.; Wang, Y.; Ryu, Y.; Chen, G.; Dong, W.; Hu, Z.; et al. Increased atmospheric vapor pressure deficit reduces global vegetation growth. *Sci. Adv.* **2019**, *5*, eaax1396. [CrossRef]
5. Schuldt, B.; Buras, A.; Arend, M.; Vitasse, Y.; Beierkuhnlein, C.; Damm, A.; Gharun, M.; Grams, T.E.E.; Hauck, M.; Hajek, P.; et al. A first assessment of the impact of the extreme 2018 summer drought on Central European forests. *Basic Appl. Ecol.* **2020**. [CrossRef]
6. Kovats, R.S.; Valentini, R.; Bouwer, L.M.; Georgopoulou, E.; Jacob, D.; Martin, E.; Rounsevell, M.; Soussana, J.-F. Impacts, Adaptation, and Vulnerability. Part B: Regional Aspects. *Clim. Chang.* **2014**, *2014*, 1267–1326.

7. Rathgeber, C.B.K.; Fonti, P.; Shishov, V.V.; Rozenberg, P. Wood formation and tree adaptation to climate. *Ann. For. Sci.* **2019**, *76*, 10–12. [CrossRef]

8. Badeck, F.-W.; Bondeau, A.; Bottcher, K.; Doktor, D.; Lucht, W.; Schaber, J.; Sitch, S. Responses of spring phenology to climate change. *New Phytol.* **2004**, *162*, 295–309. [CrossRef]

9. Donnelly, A.; Jones, M.; Sweeney, J. A review of indicators of climate change for use in Ireland. *Int. J. Biometeorol.* **2004**, *49*. [CrossRef]

10. Gričar, J.; Prislan, P.; Gryc, V.; Vavrčík, H.; De Luis, M.; Čufar, K. Plastic and locally adapted phenology in cambial seasonality and production of xylem and phloem cells in Picea abies from temperate environments. *Tree Physiol.* **2014**, *34*, 869–881. [CrossRef]

11. Vieira, J.; Moura, M.; Nabais, C.; Freitas, H.; Campelo, F. Seasonal adjustment of primary and secondary growth in maritime pine under simulated climatic changes. *Ann. For. Sci.* **2019**, *76*, 84. [CrossRef]

12. Plomion, C.; Leprovost, G.; Stokes, A. Wood Formation in Trees Wood Formation in Trees. *Plant Physiol.* **2001**, *127*, 1513–1523. [CrossRef] [PubMed]

13. Chmielewski, F.M.; Rotzer, T. Response of tree phenology to climate change across Europe. *Agric. For. Meteorol.* **2001**, *108*, 101–112. [CrossRef]

14. Čufar, K.; Prislan, P.; De Luis, M.; Gričar, J. Tree-ring variation, wood formation and phenology of beech (*Fagus sylvatica*) from a representative site in Slovenia, SE Central Europe. *Trees-Struct. Funct.* **2008**, *22*, 749–758. [CrossRef]

15. Rossi, S.; Deslauriers, A.; Gričar, J.; Seo, J.W.; Rathgeber, C.B.K.; Anfodillo, T.; Morin, H.; Levanic, T.; Oven, P.; Jalkanen, R. Critical temperatures for xylogenesis in conifers of cold climates. *Glob. Ecol. Biogeogr.* **2008**, *17*, 696–707. [CrossRef]

16. Moser, L.; Fonti, P.; Buntgen, U.; Esper, J.; Luterbacher, J.; Franzen, J.; Frank, D. Timing and duration of European larch growing season along altitudinal gradients in the Swiss Alps. *Tree Physiol.* **2010**, *30*, 225–233. [CrossRef]

17. Martinez del Castillo, E.; Longares, L.A.; Gričar, J.; Prislan, P.; Gil-Pelegrín, E.; Čufar, K.; de Luis, M. Living on the Edge: Contrasted Wood-Formation Dynamics in *Fagus sylvatica* and *Pinus sylvestris* under Mediterranean Conditions. *Front. Plant Sci.* **2016**, *7*, 370. [CrossRef]

18. Saderi, S.; Rathgeber, C.B.K.; Rozenberg, P.; Fournier, M. Phenology of wood formation in larch (Larix decidua Mill.) trees growing along a 1000-m elevation gradient in the French Southern Alps. *Ann. For. Sci.* **2019**, *76*, 89. [CrossRef]

19. Lundqvist, S.-O.; Seifert, S.; Grahn, T.; Olsson, L.; García-Gil, M.R.; Karlsson, B.; Seifert, T. Age and weather effects on between and within ring variations of number, width and coarseness of tracheids and radial growth of young Norway spruce. *Eur. J. For. Res.* **2018**, *137*, 719–743. [CrossRef]

20. Rathgeber, C.B.K.; Cuny, H.E.; Fonti, P. Biological Basis of Tree-Ring Formation: A Crash Course. *Front. Plant Sci.* **2016**, *7*, 734. [CrossRef]

21. Prislan, P.; Gričar, J.; de Luis, M.; Smith, K.T.; Čufar, K. Phenological variation in xylem and phloem formation in *Fagus sylvatica* from two contrasting sites. *Agric. For. Meteorol.* **2013**, *180*, 142–151. [CrossRef]

22. Rossi, S.; Deslauriers, A.; Anfodillo, T.; Morin, H.; Saracino, A.; Motta, R.; Borghetti, M. Conifers in cold environments synchronize maximum growth rate of tree-ring formation with day length. *New Phytol.* **2006**, *170*, 301–310. [CrossRef] [PubMed]

23. Rathgeber, C.B.K.; Rossi, S.; Bontemps, J.D. Cambial activity related to tree size in a mature silver-fir plantation. *Ann. Bot.* **2011**, *108*, 429–438. [CrossRef] [PubMed]

24. Rossi, S.; Deslauriers, A.; Anfodillo, T.; Carrer, M. Age-dependent xylogenesis in timberline conifers. *New Phytol.* **2008**, *177*, 199–208. [CrossRef]

25. Vitasse, Y.; Delzon, S.; Bresson, C.C.; Michalet, R.; Kremer, A. Altitudinal differentiation in growth and phenology among populations of temperate-zone tree species growing in a common garden. *Can. J. For. Res.* **2009**, *39*, 1259–1269. [CrossRef]

26. Cuny, H.E.; Rathgeber, C.B.K.; Kiessé, T.S.; Hartmann, F.P.; Barbeito, I.; Fournier, M. Generalized additive models reveal the intrinsic complexity of wood formation dynamics. *J. Exp. Bot.* **2013**, *64*, 1983–1994. [CrossRef]

27. Klimo, E.; Hager, H.; Kulhavy, J. *Spruce Monocultures in Central Europe—Problems and Prospects*; European Forest Institute: Joensuu, Finland, 2000.

28. Pugh, T.A.M.; Lindeskog, M.; Smith, B.; Poulter, B.; Arneth, A.; Haverd, V.; Calle, L. Role of forest regrowth in global carbon sink dynamics. *Proc. Natl. Acad. Sci. USA* **2019**, *116*, 4382–4387. [CrossRef]

29. Bouriaud, O.; Popa, I. Comparative dendroclimatic study of Scots pine, Norway spruce, and silver fir in the Vrancea Range, Eastern Carpathian Mountains. *Trees-Struct. Funct.* **2009**, *23*, 95–106. [CrossRef]

30. van der Maaten-Theunissen, M.; Kahle, H.-P.; van der Maaten, E. Drought sensitivity of Norway spruce is higher than that of silver fir along an altitudinal gradient in southwestern Germany. *Ann. For. Sci.* **2013**, *70*, 185–193. [CrossRef]

31. Bohn, U.; Neuhäusl, R.; Gollub, G.; Hettwer, C.; Neuhäuslova, Z.; Schlüter, H.; Weber, H. *Map of the Natural Vegetation of Europe 1: 2,500,000, Map and Explanatory Text*; Landwirtschaftsverlag: Münster, Germany, 2003.

32. Kandler, O. Development of the Recent Episode of Tannensterben (Fir Decline) in Eastern Bavaria and the Bavarian Alps. In *Forest Decline in the Atlantic and Pacific Region*; Hüttl, R.F., Mueller-Dombois, D., Eds.; Springer: Berlin/Heidelberg, Germany, 1993; pp. 216–226.

33. Larsen, J.B. Das Tannensterben: Eine neue Hypothese zur Klärung des Hintergrundes dieser rätselhaften Komplexkrankheit der Weißtanne (Abies alba Mill.). *Forstwiss. Cent.* **1986**, *105*, 381–396. [CrossRef]

34. Meining, S.; Puhlmann, H.; Augustin, N. *Waldzustandsbericht 2016 für Baden-Württemberg*; Forstl. Versuchs- und Forschungsanstalt Baden-württemb: Breisgau, Germany, 2016.

35. BMEL. *Wald und Rohholzpotenzial der Nächsten 40 Jahre*; BMEL: Berlin, Germany, 2016.

36. Dolos, K.; Märkel, U. *Modellierung der Klimatischen Standorteignung Forstlich Relevanter Baumarten*; LUBW Klimopass-Berichte: Karlsruhe, Germany, 2016.

37. Antonucci, S.; Rossi, S.; Lombardi, F.; Marchetti, M.; Tognetti, R. Influence of climatic factors on silver fir xylogenesis along the Italian Peninsula. *IAWA J.* **2019**, *40*, 259–275. [CrossRef]

38. Cuny, H.E.; Rathgeber, C.B.K.; Lebourgeois, F.; Fortin, M.; Fournier, M. Life strategies in intra-annual dynamics of wood formation: Example of three conifer species in a temperate forest in north-east France. *Tree Physiol.* **2012**, *32*, 612–625. [CrossRef] [PubMed]

39. Reif, A.; Brucker, U.; Kratzer, R.; Schmiedinger, A.; Bauhus, J. Waldbau und Baumartenwahl in Zeiten des Klimawandels aus Sicht des Naturschutzes. *BfN-Skripten* **2010**, *272*, 125.

40. Lebourgeois, F.; Rathgeber, C.B.K.; Ulrich, E. Sensitivity of French temperate coniferous forests to climate variability and extreme events (Abies alba, Picea abies and *Pinus sylvestris*). *J. Veg. Sci.* **2010**, *21*, 364–376. [CrossRef]

41. Eilmann, B.; Zweifel, R.; Buchmann, N.; Graf Pannatier, E.; Rigling, A. Drought alters timing, quantity, and quality of wood formation in Scots pine. *J. Exp. Bot.* **2011**, *62*, 2763–2771. [CrossRef] [PubMed]

42. Bigler, C.; Bräker, O.U.; Bugmann, H.; Dobbertin, M.; Rigling, A. Drought as an inciting mortality factor in scots pine stands of the Valais, Switzerland. *Ecosystems* **2006**, *9*, 330–343. [CrossRef]

43. Swidrak, I.; Gruber, A.; Oberhuber, W. Xylem and phloem phenology in co-occurring conifers exposed to drought. *Trees* **2014**, *28*, 1161–1171. [CrossRef]

44. del Castillo, E.M.; Prislan, P.; Gričar, J.; Gryc, V.; Merela, M.; Giagli, K.; de Luis, M.; Vavrčík, H.; Čufar, K. Emerging challenges for beech and co-occuring conifers in a changing climate context. *Dendrochronologia* **2018**, *52*, 1–10. [CrossRef]

45. Ellenberg, H.; Leuschner, C. *Vegetation Mitteleuropas Mit den Alpen: In Ökologischer, Dynamischer und Historischer Sicht*, 5th ed.; UTB: Stuttgart, Germany, 2010.

46. Prislan, P.; Gričar, J.; Čufar, K.; de Luis, M.; Merela, M.; Rossi, S. Growing season and radial growth predicted for *Fagus sylvatica* under climate change. *Clim. Chang.* **2019**, *153*, 181–197. [CrossRef]

47. Scharnweber, T.; Manthey, M.; Criegee, C.; Bauwe, A.; Schröder, C.; Wilmking, M. Drought matters—Declining precipitation influences growth of *Fagus sylvatica* L. and *Quercus robur* L. in north-eastern Germany. *For. Ecol. Manag.* **2011**, *262*, 947–961. [CrossRef]

48. Giagli, K.; Gričar, J.; Vavrčík, H.; Menšík, L.; Gryc, V. The effects of drought on wood formation in *Fagus sylvatica* during two contrasting years. *IAWA J.* **2016**, *37*, 332–348. [CrossRef]

49. van der Werf, G.W.; Sass-Klaassen, U.; Mohren, G.M.J. The impact of the 2003 summer drought on the intra-annual growth pattern of beech (*Fagus sylvatica* L.) and oak (*Quercus robur* L.) on a dry site in the Netherlands. *Dendrochronologia* **2007**, *25*, 103–112. [CrossRef]

50. Kraus, C.; Zang, C.; Menzel, A. Elevational response in leaf and xylem phenology reveals different prolongation of growing period of common beech and Norway spruce under warming conditions in the Bavarian Alps. *Eur. J. For. Res.* **2016**, *135*, 1011–1023. [CrossRef]

51. Legendre, L.; Legendre, P. *Numerical Ecology*, 3rd ed.; Elsevier: Amsterdam, The Netherlands, 2012.

52. Jarvis, A.; Reuter, H.I.; Nelson, A.; Guevara, E. Hole-filled seamless SRTM data V4, International Centre for Tropical Agriculture (CIAT). 2008. Available online: http://srtm.csi.cgiar.org (accessed on 1 December 2020).

53. Schrödter, H. *Verdunstung: Anwendungsorientierte Messverfahren und Bestimmungsmethoden*; Springer: Berlin/Heidelberg, Germany, 2013.

54. Dietrich, H.; Wolf, T.; Kawohl, T.; Wehberg, J.; Kändler, G.; Mette, T.; Röder, A.; Böhner, J. Temporal and spatial high-resolution climate data from 1961 to 2100 for the German National Forest Inventory (NFI). *Ann. For. Sci.* **2019**, *76*, 6. [CrossRef]

55. Nothdurft, A.; Wolf, T.; Ringeler, A.; Böhner, J.; Saborowski, J. Spatio-temporal prediction of site index based on forest inventories and climate change scenarios. *For. Ecol. Manag.* **2012**, *279*, 97–111. [CrossRef]

56. Hanewinkel, M.; Cullmann, D.; Schelhaas, M.-J.; Nabuurs, G.-J.; Zimmermann, N. Climate change may cause severe loss in the economic value of European forest land. *Nat. Clim. Chang.* **2013**, *3*, 203–207. [CrossRef]

57. Baier, P.; Pennerstorfer, J.; Schopf, A. PHENIPS—A comprehensive phenology model of Ips typographus (L.) (Col., Scolytinae) as a tool for hazard rating of bark beetle infestation. *For. Ecol. Manag.* **2007**, *249*, 171–186. [CrossRef]

58. Pasho, E.; Camarero, J.J.; de Luis, M.; Vicente-Serrano, S.M. Impacts of drought at different time scales on forest growth across a wide climatic gradient in north-eastern Spain. *Agric. For. Meteorol.* **2011**, *151*, 1800–1811. [CrossRef]

59. Agnew, C.T. Using the SPI to Identify Drought. *Drought Netw. News* **2000**, *12*, 5–12.

60. McKee, T.B.; Doesken, N.J.; Kleist, J. Drought monitoring with multiple time scales. In Proceedings of the Ninth Conference on Applied Climatology; American Meteorological Society: Boston, MA, USA, 1995; pp. 233–236.

61. McMaster, G.S.; Wilhelm, W.W. Growing degree-days: One equation, two interpretations. *Agric. For. Meteorol.* **1997**, *87*, 291–300. [CrossRef]

62. Rossi, S.; Anfodillo, T.; Menardi, R. Trephor: A new tool for sampling microcores from tree stems. *IAWA J.* **2006**, *27*, 89–97. [CrossRef]

63. Gärtner, H.; Lucchinetti, S.; Schweingruber, F.H. New perspectives for wood anatomical analysis in dendrosciences: The GSL1-microtome. *Dendrochronologia* **2014**, *32*, 47–51. [CrossRef]

64. Deslauriers, A.; Rossi, S.; Liang, E. Collecting and Processing Wood Microcores for Monitoring Xylogenesis. In *Plant Microtechniques and Protocols*; Springer International Publishing: Cham, Switzerland, 2015; pp. 417–429. ISBN 9783319199443.

65. De Micco, V.; Carrer, M.; Rathgeber, C.B.K.; Camarero, J.J.; Voltas, J.; Cherubini, P.; Battipaglia, G. From xylogenesis to tree-rings: Wood traits to investigate tree response to environmental changes. *IAWA J.* **2019**, *40*, 155–182. [CrossRef]

66. Rossi, S.; Deslauriers, A.; Anfodillo, T. Assessment of cambial activity and xylogenesis by microsampling tree species: An example at the Alpine timberline. *IAWA J.* **2006**, *27*, 383–394. [CrossRef]

67. Frankenstein, C.; Eckstein, D.; Schmitt, U. The onset of cambium activity—A matter of agreement? *Dendrochronologia* **2005**, *23*, 57–62. [CrossRef]

68. Delpierre, N.; Lireux, S.; Hartig, F.; Camarero, J.J.; Cheaib, A.; Čufar, K.; Cuny, H.E.; Deslauriers, A.; Fonti, P.; Gričar, J.; et al. Chilling and forcing temperatures interact to predict the onset of wood formation in Northern Hemisphere conifers. *Glob. Chang. Biol.* **2019**, *25*, 1089–1105. [CrossRef]

69. Stangler, D.F.; Mann, M.; Kahle, H.-P.; Rosskopf, E.; Fink, S.; Spiecker, H. Spatiotemporal alignment of radial tracheid diameter profiles of submontane Norway spruce. *Dendrochronologia* **2016**, *37*, 33–45. [CrossRef]

70. Pya, N.; Wood, S.N. Shape constrained additive models. *Stat. Comput.* **2015**, *25*, 543–559. [CrossRef]

71. R Core Team. R Programming Language. Available online: http://www.r-project.org (accessed on 1 December 2020).

72. Lloret, F.; Keeling, E.G.; Sala, A. Components of tree resilience: Effects of successive low-growth episodes in old ponderosa pine forests. *Oikos* **2011**, *120*, 1909–1920. [CrossRef]

73. Schabenberger, O.; Pierce, F.J. *Contemporary Statistical Models for the Plant and Soil Sciences*; CRC Press: Boca Raton, FL, USA, 2001.

74. Bates, D.; Mächler, M.; Bolker, B.M.; Walker, S.C. Fitting linear mixed-effects models using lme4. *J. Stat. Softw.* **2015**, *67*, 1–48. [CrossRef]

75. Lenth, R.; Singmann, H.; Love, J.; Buerkner, P.; Herve, M. Emmeans: Estimated Marginal Means, Aka Least-Squares Means. R Package Version 1.4.5. Available online: https://github.com/rvlenth/emmeans (accessed on 28 November 2020).

76. Kuznetsova, A.; Brockhoff, P.B.; Christensen, R.H.B. lmerTest Package: Tests in Linear Mixed Effects Models. *J. Stat. Softw.* **2017**, *82*, 1–26. [CrossRef]

77. Emerson, J.W.; Green, W.A.; Schloerke, B.; Crowley, J.; Cook, D.; Hofmann, H.; Wickham, H. The Generalized Pairs Plot. *J. Comput. Graph. Stat.* **2013**, *22*, 79–91. [CrossRef]

78. Ren, P.; Rossi, S.; Camarero, J.J.; Ellison, A.M.; Liang, E.; Peñuelas, J. Critical temperature and precipitation thresholds for the onset of xylogenesis of Juniperus przewalskii in a semi-arid area of the north-eastern Tibetan Plateau. *Ann. Bot.* **2018**, *121*, 617–624. [CrossRef] [PubMed]

79. Gruber, A.; Strobl, S.; Veit, B.; Oberhuber, W. Impact of drought on the temporal dynamics of wood formation in *Pinus sylvestris*. *Tree Physiol.* **2010**, *30*, 490–501. [CrossRef] [PubMed]

80. Rossi, S.; Girard, M.J.; Morin, H. Lengthening of the duration of xylogenesis engenders disproportionate increases in xylem production. *Glob. Chang. Biol.* **2014**, *20*, 2261–2271. [CrossRef] [PubMed]

81. Oribe, Y.; Funada, R.; Shibagaki, M.; Kubo, T. Cambial reactivation in locally heated stems of the evergreen conifer Abies sachalinensis (Schmidt) masters. *Planta* **2001**, *212*, 684–691. [CrossRef]

82. Begum, S.; Kudo, K.; Rahman, M.H.; Nakaba, S.; Yamagishi, Y.; Nabeshima, E.; Nugroho, W.D.; Oribe, Y.; Kitin, P.; Jin, H.O.; et al. Climate change and the regulation of wood formation in trees by temperature. *Trees-Struct. Funct.* **2018**, *32*, 3–15. [CrossRef]

83. Swidrak, I.; Gruber, A.; Kofler, W.; Oberhuber, W. Effects of environmental conditions on onset of xylem growth in *Pinus sylvestris* under drought. *Tree Physiol.* **2011**, *31*, 483–493. [CrossRef]

84. Rossi, S.; Morin, H.; Deslauriers, A.; Plourde, P.Y. Predicting xylem phenology in black spruce under climate warming. *Glob. Chang. Biol.* **2011**, *17*, 614–625. [CrossRef]

85. Rossi, S.; Anfodillo, T.; Čufar, K.; Cuny, H.E.; Deslauriers, A.; Fonti, P.; Frank, D.; Gričar, J.; Gruber, A.; Huang, J.G.; et al. Pattern of xylem phenology in conifers of cold ecosystems at the Northern Hemisphere. *Glob. Chang. Biol.* **2016**, *22*, 3804–3813. [CrossRef]

86. Gričar, J.; Zupancic, M.; Čufar, K.; Koch, G.; Schmitt, U.; Oven, P. Effect of local heating and cooling on cambial activity and cell differentiation in the stem of Norway spruce (Picea abies). *Ann. Bot.* **2006**, *97*, 943–951. [CrossRef] [PubMed]

87. Gričar, J.; Zupančič, M.; Čufar, K.; Oven, P. Regular cambial activity and xylem and phloem formation in locally heated and cooled stem portions of Norway spruce. *Wood Sci. Technol.* **2007**, *41*, 463–475. [CrossRef]

88. Oribe, Y.; Kubo, T. Effect of heat on cambial reactivation during winter dormancy in evergreen and deciduous conifers. *Tree Physiol.* **1997**, *17*, 81–87. [CrossRef] [PubMed]

89. Capdevielle-Vargas, R.; Estrella, N.; Menzel, A. Multiple-year assessment of phenological plasticity within a beech (*Fagus sylvatica* L.) stand in southern Germany. *Agric. For. Meteorol.* **2015**, *211–212*, 13–22. [CrossRef]

90. Patel, V.R.; Pramod, S.; Rao, K.S. Cambial activity, annual rhythm of xylem production in relation to phenology and climatic factors and lignification pattern during xylogenesis in drum-stick tree (Moringa oleifera). *Flora-Morphol. Distrib. Funct. Ecol. Plants* **2014**, *209*, 556–566. [CrossRef]

91. Chen, L.; Rossi, S.; Deslauriers, A.; Liu, J. Contrasting strategies of xylem formation between black spruce and balsam fir in Quebec, Canada. *Tree Physiol.* **2019**, *39*, 747–754. [CrossRef]

92. Huang, J.; Ma, Q.; Rossi, S.; Biondi, F.; Deslauriers, A.; Fonti, P.; Liang, E.; Mäkinen, H.; Oberhuber, W.; Rathgeber, C.B.K.; et al. Photoperiod and temperature as dominant environmental drivers triggering secondary growth resumption in Northern Hemisphere conifers. *Proc. Natl. Acad. Sci. USA* **2020**, *117*, 20645–20652. [CrossRef]

93. Vitasse, Y.; Signarbieux, C.; Fu, Y.H. Global warming leads to more uniform spring phenology across elevations. *Proc. Natl. Acad. Sci. USA* **2018**, *115*, 1004–1008. [CrossRef]

94. Prislan, P.; Gričar, J.; de Luis, M.; Novak, K.; Martinez del Castillo, E.; Schmitt, U.; Koch, G.; Štrus, J.; Mrak, P.; Žnidarič, M.T.; et al. Annual Cambial Rhythm in Pinus halepensis and *Pinus sylvestris* as Indicator for Climate Adaptation. *Front. Plant Sci.* **2016**, *7*, 1923. [CrossRef]

95. Malik, R.; Rossi, S.; Sukumar, R. Variations in the timing of different phenological stages of cambial activity in Abies pindrow (Royle) along an elevation gradient in the north-western Himalaya. *Dendrochronologia* **2020**, *59*, 125660. [CrossRef]

96. Prislan, P.; Koch, G.; Čufar, K.; Gričar, J.; Schmitt, U. Topochemical investigations of cell walls in developing xylem of beech (*Fagus sylvatica* L.). *Holzforschung* **2009**, *63*. [CrossRef]

97. Rossi, S.; Morin, H.; Deslauriers, A. Causes and correlations in cambium phenology: Towards an integrated framework of xylogenesis. *J. Exp. Bot.* **2012**, *63*, 2117–2126. [CrossRef]

98. Rossi, S.; Anfodillo, T.; Čufar, K.; Cuny, H.E.; Deslauriers, A.; Fonti, P.; Frank, D.; Gričar, J.; Gruber, A.; King, G.; et al. A meta-analysis of cambium phenology and growth: Linear and non-linear patterns in conifers of the northern hemisphere. *Ann. Bot.* **2013**, *112*, 1911–1920. [CrossRef]

99. Fonti, P.; Von Arx, G.; García-González, I.; Eilmann, B.; Sass-Klaassen, U.; Gärtner, H.; Eckstein, D. Studying global change through investigation of the plastic responses of xylem anatomy in tree rings. *New Phytol.* **2010**, *185*, 42–53. [CrossRef]

100. Prislan, P.; Čufar, K.; De Luis, M.; Gričar, J. Precipitation is not limiting for xylem formation dynamics and vessel development in European beech from two temperate forest sites. *Tree Physiol.* **2018**, *38*, 186–197. [CrossRef] [PubMed]

101. Sass, U.; Eckstein, D. The variability of vessel size in beech (*Fagus sylvatica* L.) and its ecophysiological interpretation. *Trees* **1995**, *9*, 247–252. [CrossRef]

102. Wagenführ, R. *Holzatlas*; Fachbuchverlag: Leipzig, Germany, 1996.

103. Cuny, H.E.; Rathgeber, C.B.K.; Frank, D.; Fonti, P.; Fournier, M. Kinetics of tracheid development explain conifer tree-ring structure. *New Phytol.* **2014**, *203*, 1231–1241. [CrossRef] [PubMed]

104. Andrianantenaina, A.; Rathgeber, C.B.K.; Pérez-de-Lis, G.; Cuny, H.E.; Ruelle, J. Quantifying intra-annual dynamics of carbon sequestration in the forming wood: A novel histologic approach. *Ann. For. Sci.* **2019**, *76*, 62. [CrossRef]

105. Oladi, R.; Pourtahmasi, K.; Eckstein, D.; Bräuning, A. Seasonal dynamics of wood formation in Oriental beech (Fagus orientalis Lipsky) along an altitudinal gradient in the Hyrcanian forest, Iran. *Trees-Struct. Funct.* **2011**, *25*, 425–433. [CrossRef]

106. Cuny, H.E.; Fonti, P.; Rathgeber, C.B.K.; Arx, G.; Peters, R.L.; Frank, D.C. Couplings in cell differentiation kinetics mitigate air temperature influence on conifer wood anatomy. *Plant. Cell Environ.* **2019**, *42*, 1222–1232. [CrossRef]

107. Cuny, H.E.; Rathgeber, C.B.K. Xylogenesis: Coniferous Trees of Temperate Forests Are Listening to the Climate Tale during the Growing Season But Only Remember the Last Words! *Plant Physiol.* **2016**, *171*, 306–317. [CrossRef] [PubMed]

108. Larcher, W. *Physiological Plant Ecology: Ecophysiology and Stress Physiology of Functional Groups*; Springer Science & Business Media: Berlin/Heidelberg, Germany, 2003; ISBN 9783540435167.

109. Fernández-de-Uña, L.; Rossi, S.; Aranda, I.; Fonti, P.; González-González, B.D.; Cañellas, I.; Gea-Izquierdo, G. Xylem and Leaf Functional Adjustments to Drought in *Pinus sylvestris* and Quercus pyrenaica at Their Elevational Boundary. *Front. Plant Sci.* **2017**, *8*, 1200. [CrossRef] [PubMed]

110. Aranda, I.; Cano, F.J.; Gasco, A.; Cochard, H.; Nardini, A.; Mancha, J.A.; Lopez, R.; Sanchez-Gomez, D. Variation in photosynthetic performance and hydraulic architecture across European beech (*Fagus sylvatica* L.) populations supports the case for local adaptation to water stress. *Tree Physiol.* **2015**, *35*, 34–46. [CrossRef] [PubMed]

111. Camarero, J.J.; Gazol, A.; Sangüesa-Barreda, G.; Oliva, J.; Vicente-Serrano, S.M. To die or not to die: Early warnings of tree dieback in response to a severe drought. *J. Ecol.* **2015**, *103*, 44–57. [CrossRef]

112. Martínez-Sancho, E.; Vásconez Navas, L.K.; Seidel, H.; Dorado-Liñán, I.; Menzel, A. Responses of Contrasting Tree Functional Types to Air Warming and Drought. *Forests* **2017**, *8*, 450. [CrossRef]

113. Lebourgeois, F.; Gomez, N.; Pinto, P.; Mérian, P. Mixed stands reduce Abies alba tree-ring sensitivity to summer drought in the Vosges mountains, western Europe. *For. Ecol. Manag.* **2013**, *303*, 61–71. [CrossRef]

114. Liu, X.; Wang, C.; Zhao, J. Seasonal Drought Effects on Intra-Annual Stem Growth of Taiwan Pine along an Elevational Gradient in Subtropical China. *Forests* **2019**, *10*, 1128. [CrossRef]

115. Michelot, A.; Simard, S.; Rathgeber, C.B.K.; Dufrêsne, E.; Damesin, C. Comparing the intra-annual wood formation of three European species (*Fagus sylvatica*, Quercus petraea and *Pinus sylvestris*) as related to leaf phenology and non-structural carbohydrate dynamics. *Tree Physiol.* **2012**, *32*, 1033–1045. [CrossRef]

116. Jyske, T.; Mäkinen, H.; Kalliokoski, T.; Nöjd, P. Intra-annual tracheid production of Norway spruce and Scots pine across a latitudinal gradient in Finland. *Agric. For. Meteorol.* **2014**, *194*, 241–254. [CrossRef]

117. Zhang, J.; Gou, X.; Manzanedo, R.D.; Zhang, F.; Pederson, N. Cambial phenology and xylogenesis of Juniperus przewalskii over a climatic gradient is influenced by both temperature and drought. *Agric. For. Meteorol.* **2018**, *260–261*, 165–175. [CrossRef]

118. Lupi, C.; Morin, H.; Deslauriers, A.; Rossi, S. Xylogenesis in black spruce: Does soil temperature matter? *Tree Physiol.* **2012**, *32*, 74–82. [CrossRef] [PubMed]

119. Ren, P.; Ziaco, E.; Rossi, S.; Biondi, F.; Prislan, P.; Liang, E. Growth rate rather than growing season length determines wood biomass in dry environments. *Agric. For. Meteorol.* **2019**, *271*, 46–53. [CrossRef]

120. Kahle, H.-P. Impact of the drought in 2003 on intra- and inter-annual stem radial growth of beech and spruce along an altitudinal gradient in the Black Forest, Germany. *Tree Rings Archeol. Clim. Ecol.* **2006**, *4*, 151–163.

121. Gričar, J.; Čufar, K. Seasonal dynamics of phloem and xylem formation in silver fir and Norway spruce as affected by drought. *Russ. J. Plant Physiol.* **2008**, *55*, 538–543. [CrossRef]

122. Balducci, L.; Cuny, H.E.; Rathgeber, C.B.K.; Deslauriers, A.; Giovannelli, A.; Rossi, S. Compensatory mechanisms mitigate the effect of warming and drought on wood formation. *Plant. Cell Environ.* **2016**, *39*, 1338–1352. [CrossRef]

123. Camarero, J.J.; Olano, J.M.; Parras, A. Plastic bimodal xylogenesis in conifers from continental Mediterranean climates. *New Phytol.* **2010**, *185*, 471–480. [CrossRef]

124. Maxime, C.; Hendrik, D. Effects of climate on diameter growth of co-occurring *Fagus sylvatica* and Abies alba along an altitudinal gradient. *Trees-Struct. Funct.* **2011**, *25*, 265–276. [CrossRef]

125. Mattes, A. Zuwachs und Konkurrenz in Buchen-/Eichenmischbeständen unter sich Ändernden Klimabedingungen. Ph.D. Thesis, Albert-Ludwigs-Universität Freiburg, Breisgau, Germany, 2014.

126. Vitali, V.; Büntgen, U.; Bauhus, J. Silver fir and Douglas fir are more tolerant to extreme droughts than Norway spruce in south-western Germany. *Glob. Chang. Biol.* **2017**, *23*, 5108–5119. [CrossRef]

127. Marion, L.; Gričar, J.; Oven, P. Wood formation in urban Norway maple trees studied by the micro-coring method. *Dendrochronologia* **2007**, *25*, 97–102. [CrossRef]

128. Oribe, Y.; Funada, R.; Kubo, T. Relationships between cambial activity, cell differentiation and the localization of starch in storage tissues around the cambium in locally heated stems of Abies sachalinensis (Schmidt) Masters. *Trees* **2003**, *17*, 185–192. [CrossRef]

129. Oberhuber, W.; Gruber, A. Climatic influences on intra-annual stem radial increment of *Pinus sylvestris* (L.) exposed to drought. *Trees-Struct. Funct.* **2010**, *24*, 887–898. [CrossRef] [PubMed]

130. Camarero, J.J.; Gazol, A.; Sangüesa-Barreda, G.; Cantero, A.; Sánchez-Salguero, R.; Sánchez-Miranda, A.; Granda, E.; Serra-Maluquer, X.; Ibáñez, R. Forest growth responses to drought at short- and long-term scales in Spain: Squeezing the stress memory from tree rings. *Front. Ecol. Evol.* **2018**, *6*. [CrossRef]

131. Eilmann, B.; Rigling, A. Tree-growth analyses to estimate tree species ' drought tolerance. *Tree Physiol.* **2012**, *32*, 178–187. [CrossRef] [PubMed]

132. John, R.; Grüner, J.; Seitz, G.; Delb, H. *Buchen in Südwestdeutschland Leiden unter dem Trockenstress der Vorjahre*; FVA Waldschutz-INFO: Freiburg, Germany, 2019.